Pesticide fate at catchment scale: conceptual modelling of stream CSIA data

Stefanie R. Lutz[1], Ype van der Velde[2], Omniea F. Elsayed[3], Gwenaël Imfeld[3], Marie Lefrancq[3], Sylvain Payraudeau[3], Boris M. van Breukelen[4]

[1]UFZ Helmholtz Centre for Environmental Research, Department Catchment Hydrology, Theodor-Lieser-Str. 4, 06120 Halle (Saale), Germany

[2]Department of Earth Sciences, Faculty of Earth and Life Sciences, VU University Amsterdam, De Boelelaan 1085, 1081 HV Amsterdam, The Netherlands

[3]Laboratoire d'hydrologie et de Géochimie de Strasbourg (LHyGeS), Université de Strasbourg/ENGEES, 1 rue Blessig, 67084 Strasbourg cedex, France

[4]Delft University of Technology, Faculty of Civil Engineering and Geosciences, Department of Water Management, Stevinweg 1, Delft, The Netherlands

Correspondence to: Stefanie R. Lutz (stefanie.lutz@ufz.de)

Abstract. Compound-specific stable isotope analysis (CSIA) has proven beneficial in the characterization of contaminant degradation in groundwater, but it has never been used to assess pesticide transformation at catchment scale. This study presents concentration and carbon CSIA data of the herbicides S-metolachlor and acetochlor from three locations (plot, drain, and catchment outlets) in a 47-ha agricultural catchment (Bas-Rhin France). Herbicide concentrations at the catchment outlet were highest (62 µg L^{-1}) in response to an intense rainfall event following herbicide application. Increasing $\delta^{13}C$-values of S-metolachlor and acetochlor by more than 2 ‰ during the study period indicated herbicide degradation. To assist the interpretation of these data, discharge, concentrations and $\delta^{13}C$-values of S-metolachlor were modelled with a conceptual mathematical model using the transport formulation by travel time distributions. Testing of different model setups supported the assumption that degradation half-lives (DT50) increase with increasing soil depth, which can be straightforwardly implemented in conceptual models using travel time distributions. Moreover, model calibration yielded an estimate of a field-integrated isotopic enrichment factor as opposed to laboratory-based assessments of enrichment factors in closed systems. Thirdly, the Rayleigh equation commonly applied in groundwater studies was tested by our model for its potential to quantify degradation at catchment scale. It provided conservative estimates on the extent of degradation as occurred in stream samples. However, largely exceeding the simulated degradation within the entire catchment, these estimates were not representative of overall degradation at catchment scale. The conceptual modelling approach thus enabled us to upscale sample-based CSIA information on degradation to the catchment scale. Overall, this study demonstrates the benefit of combining monitoring and conceptual modelling of concentrations and CSIA data, and advocates the use of travel time distributions for assessing pesticide fate and transport at catchment scale.

1 Introduction

Diffuse pollution of groundwater and rivers is a recurrent issue in agricultural catchments due to the extensive application of pesticides to arable land. Pesticide degradation at catchment scale removes pesticides from the environment, which reduces their potential impact on the ecosystem provided that pesticide transformation products are non-toxic. However, pesticide concentrations vary not only due to degradation, but also depending on, e.g., the amount and timing of pesticide application (Battaglin and Goolsby, 1999) or the extent of dilution by pristine water (Schreglmann et al., 2013). Hence, concentration data alone cannot conclusively allow distinction between destructive (i.e., degradation) and non-destructive processes (e.g., transport and sorption). Similarly, laboratory studies allow studying specific mechanisms of pesticide degradation but hardly reflect conditions of pesticide degradation under field conditions (Fenner et al., 2013). These limitations may be overcome by compound-specific isotope analysis (CSIA), which measures the isotopic composition of the contaminant (i.e., the abundance of heavy isotopes relative to light isotopes of an element contained in the compound). The isotopic composition may change under the influence of contaminant transformation (i.e., isotope fractionation; Elsner, 2010; Schmidt and Jochmann, 2012). In contrast, non-destructive processes such as dispersion or sorption may lead to significant isotope fractionation effects only under specific conditions (Eckert et al., 2013; van Breukelen and Prommer, 2008; van Breukelen

2

and Rolle, 2012). Therefore, CSIA allows for the detection and even quantification of contaminant degradation in polluted environmental systems.

CSIA has been previously applied to study in situ degradation of organic groundwater contaminants (Blum et al., 2009; Elsner et al., 2012; Hunkeler et al., 2005; Schmidt and Jochmann, 2012; Wiegert et al., 2012; Zwank et al., 2005). In the context of diffuse agricultural pollution, CSIA has mainly been used to distinguish natural from anthropogenic nitrate sources, and discern denitrification (Divers et al., 2014; Johannsen et al., 2008; Kellman and Hillaire-Marcel, 2003; Voss et al., 2006; Wexler et al., 2014). Although CSIA may provide evidence of pesticide degradation (Fenner et al., 2013), CSIA data of pesticides remain restricted to the analysis of isotope fractionation under laboratory conditions (Hartenbach et al., 2008; Meyer and Elsner, 2013; Meyer et al., 2009; Penning et al., 2010; Reinnicke et al., 2011; Wu et al., 2014), and grab samples of groundwater and streamwater (Milosevic et al., 2013; Schreglmann et al., 2013). Degradation of chloroacetanilide herbicides and associated isotope fractionation have been recently studied in lab-scale wetlands (Elsayed et al., 2014), but CSIA of herbicides has not yet been applied at catchment scale to evaluate in situ degradation of pesticides. This study presents the first field CSIA-data of pesticides in surface runoff and streamwater from an agricultural catchment. It discusses concentration and carbon CSIA data of two chloroacetanilide herbicides (S-metolachlor and acetochlor) in a 47-ha agricultural catchment (Bas-Rhin, France) at three different locations (i.e., at the plot, drain, and catchment outlet).

In groundwater studies, CSIA-based degradation assessments have been performed by two approaches: the Rayleigh equation and reactive transport modelling. The Rayleigh equation links the measured isotope fractionation effect, via the isotope fractionation factor, to the extent of degradation (Elsner and Imfeld, 2016; Mariotti et al., 1981; Rayleigh, 1896). CSIA data and associated isotope fractionation effects have more recently been simulated using reactive transport models to characterize groundwater pollution (Atteia et al., 2008; D'Affonseca et al., 2011; Pooley et al., 2009; Prommer et al., 2009; van Breukelen et al., 2005; Wanner et al., 2012) and pesticide pollution at hillslope scale via a virtual experimental approach (Lutz et al., 2013). These models demonstrated that the Rayleigh equation systematically underestimates the extent of degradation as occurred in the analysed samples (Abe and Hunkeler, 2006; van Breukelen and Prommer, 2008; van Breukelen and Rolle, 2012).

There is a pressing need to develop reactive transport models simulating CSIA data at catchment scale in order to advance the interpretation of field isotope data of agrochemicals (Elsner and Imfeld, 2016). Therefore, the purpose of this study was to present a conceptual hydrological two-compartment model (i.e., parsimonious mathematical model) that describes pesticide transport, degradation and associated isotope fractionation in the study catchment to identify the dominant processes affecting herbicide fate and transport. The model applies the transport formulation by travel time distributions and thus aims at reconciling hydrological models with water quality models at catchment scale (Hrachowitz et al., 2016). Conceptual flow and transport modelling with travel time distributions has been recently applied at the agricultural catchment scale to simulate atrazine and chloride transport (Van der Velde et al., 2010; Benettin et al., 2013; Botter et al., 2011; Harman, 2015). The novelty of this study lies in the inclusion of CSIA data in such modelling approaches.

Finally, by comparing the model and the Rayleigh equation, this study investigates how to upscale sample-based CSIA information for degradation assessment at catchment scale. Overall, the main objectives of this study are to i) analyse herbicide CSIA data from an agricultural catchment at different scales, ii) develop a quantitative model using travel time distributions for the interpretation of pesticide concentrations and CSIA data at catchment scale, and iii) evaluate the added value of this modelling approach for the assessment of pesticide transport and degradation at catchment scale.

2 Methods

2.1 Field site description

The study was conducted in a 47-ha headwater catchment, located 30 km north of Strasbourg (Bas-Rhin, France). The catchment characteristics have been previously described in Lefrancq et al. (2017). Briefly, the mean annual temperature between 2005 and 2011 was 11.7 °C, and mean annual precipitation and potential evapotranspiration were 704 mm (±151 mm) and 820 mm (±28 mm), respectively (data from Meteo France station in Waltenheim sur Zorn at 7 km distance from the catchment). Arable land (with corn and sugar beet as main crops) comprises 88 % of the catchment area, with the remainder being roads and patches of grass. Elevation ranges between 190 m and 230 m, and the mean catchment slope is 6.7 % (±4.8 %). The main soil types are calcareous brown earth and calcic soils on hillsides, and colluvial calcic soils in the central thalweg. Soil characteristics and grain size distribution in surface soil were measured by 30 samples in the top 20 cm (clay 30.8±3.9 %, silt 61.0±4.5 %, sand 8.5±4.2 %, CaCO3 1.1±1.6 %, organic matter 2.16±0.3 %, pH KCl 6.7±0.8, phosphorus 0.11±0.04 g kg^{-1}, and CEC 15.5±1.3 cmol$^+$ kg^{-1}). Additionally, six 2-m profiles were taken, which showed a rapid decrease of organic matter with depth, from about 2.5 % on average in the top 30 cm to about 0.6 % on average at 100 to 150 cm depth. Soil characteristics were assumed homogeneous in the study area for the following analyses.

The catchment is drained by an artificial drainage network of unknown size; at least one drainpipe was active during the study and continuously discharged into the ditch close to the catchment outlet (Fig. 1).

2.2 Study compounds

This study considers the two chloroacetanilide herbicides metolachlor (2-chloro-N-(2-ethyl-6-methylphenyl)-N-(2-methoxy-1-methylethyl)acetamide) and acetochlor (2-chloro-N-(ethoxymethyl)-N-(2-ethyl-6-methylphenyl)acetamide; see section S1 and Table S1 in the supplementary material, SM). Metolachlor and acetochlor are commonly applied pesticides (Grube et al., 2011) mainly used for pre-emergence weed control. Both herbicides have been applied in the study catchment since the 1990s. In 2012, S-metolachlor (i.e., the herbicidally active S-enantiomer of metolachlor) was applied on bare soil as spray containing the commercial formulations Mercantor Gold, Dual Gold, or Camix (Syngenta). Acetochlor was applied as the commercial formulation Harness (Dow Agrosciences). According to a survey conducted among local farmers, 10.4 kg of acetochlor and 10.9 kg of S-metolachlor were applied in the catchment mainly in the first two weeks of May 2012. At the

4

experimental plot, only S-metolachlor was applied (on April 12 and May 1). We will present monitoring results for both S-metolachlor and acetochlor, but focus on S-metolachlor for the modelling.

2.3 Monitoring setup

Discharge and concentrations of S-metolachlor and acetochlor were measured between March and August 2012 at three different scales (plot experiment, drain outlet and catchment outlet). At the catchment outlet, discharge was continuously measured using a Doppler flowmeter (2150 Isco), and flow-proportional samples were taken every 20 m^3 with a refrigerated automatic sampler (Isco Avalanche). Consecutive samples were combined to composite samples; during baseflow conditions, samples were merged into weekly composite samples, whereas during runoff events, samples were merged into several composite samples according to the hydrograph components (i.e., baseflow, rising and falling limb). For the plot experiment, 77.2 m^2 were isolated on a sugar beet field with a 60 cm high shield to a depth of 30 cm below the soil surface. Surface runoff exclusively was collected in a polyethylene gutter, and discharge was measured using a Venturi channel combined with a surface water level sensor (ISMA). Flow-proportional water samples at the plot were taken every 7 L with a refrigerated automatic sampler (Isco Avalanche). Weekly grab water samples were collected from the drain outlet. Lefrancq et al. (2017) provides a more detailed description of the monitoring setup.

2.4 Concentration and CSIA analysis

Quantification and CSIA of S-metolachlor and acetochlor are described in detail elsewhere (Elsayed et al., 2014). Briefly, 1 L water samples were filtered, extracted by solid-phase extraction, concentrated under nitrogen flux to one droplet, and resuspended in 500 µL dichloromethane (DCM). Dissolved herbicides were quantified with a GC-MS/MS system with a mean uncertainty of 8 % and quantification limits of 0.05 and 0.02 µg L^{-1} for acetochlor and S-metolachlor, respectively. Herbicide concentrations were determined for 10 samples at the plot, 16 samples at the drain outlet, and 34 samples at the catchment outlet.

Carbon isotope ratios were measured in triplicates with a GC-C-IRMS system. A series of standards was dissolved in DCM to concentrations of 88.1, 35.2, 26.4, 17.6 and 3.5 µM for metolachlor resulting in a corresponding range of signal amplitudes between 120 and 7000 mV. Despite a lower reproducibility for smaller amplitude signals, the obtained values were always within 0.5 ‰ of the averaged δ^{13}C-value for the two compounds. No effect of the SPE-concentration procedure on the analytical precision could be observed.

Carbon isotope ratios ((^{13}C/^{12}C)$_{Sample}$) are reported in per mil (‰) relative to the VPDB (Vienna Pee Dee Belemnite) standard ratio ((^{13}C/^{12}C)$_{VPDB}$ = 0.0112372):

$$\delta^{13}C = \left(\frac{\left(\frac{^{13}C}{^{12}C}\right)_{Sample}}{\left(\frac{^{13}C}{^{12}C}\right)_{VPDB}} - 1 \right) \qquad (1)$$

Carbon isotope ratios of S-metolachlor were obtained for five samples at the plot and six samples at the catchment outlet (between one and nine weeks after the main application day). Additionally, the δ^{13}C-value of one S-metolachlor sample from the application tank used in the plot experiment was determined. Carbon isotope ratios of acetochlor were obtained for three samples at the plot and five samples at the catchment outlet (between two and six weeks after the main application day). No δ^{13}C-values of either herbicide were obtained for the drain outlet due to concentrations of below 0.5 µg L^{-1}.

2.5 Hydrological model and travel time distributions

The conceptual hydrological model comprises two storage reservoirs: a source zone reservoir representing the upper soil layer onto which the pesticide is applied, and a lower transport zone comprising both unsaturated soil and groundwater (Fig. 2; cf. Benettin et al., 2013; Bertuzzo et al., 2013). The source zone reservoir (S_{sz}) is fed by precipitation (P) and the transport zone (S_{tz}) is fed by recharge from the source zone reservoir (R_{tz}). Water in the source zone storage can leave the storage as evapotranspiration (E_{sz}) or discharge (Q_{sz}). Q_{sz} is zero as long as storage is below the capacity of the source zone storage. If the latter is reached, discharge from the source zone is partitioned into recharge to the transport zone (R_{tz}) and direct overland flow to the catchment outlet (OF). Overland flow is assumed to occur when the infiltration rate exceeds the infiltration capacity. This infiltration capacity is specified by a normal distribution (with mean infiltration capacity μ_{OF} and standard deviation σ_{OF} as model parameters) to reflect spatial heterogeneity of infiltration processes. This is necessary as overland flow was observed to occur under both large and much smaller rainfall events, which would not be adequately captured by a single infiltration capacity. Output fluxes from the transport zone are evapotranspiration (E_{tz}) and discharge to the catchment outlet (Q_{tz}); Q_{tz} was assumed to be a function of storage solely (S_{tz}; cf. Kirchner, 2009). Vegetation effects were not modelled. Discharge at the catchment outlet was simulated on a daily time step. The detailed equations of storage and fluxes for the hydrological model are given in Table 1.

Our model uses the transport formulation by travel time distributions, which characterize flow dynamics within a reservoir by giving the probability density function of the time that a water parcel spends inside the reservoir before leaving *via* discharge (Q) or evapotranspiration (ET), respectively (Botter et al., 2010; Hrachowitz et al., 2015; van der Velde et al., 2012). Travel time distributions also allow for the calculation of solute concentrations by convolution of travel time distributions with a relation between travel times and concentrations (Benettin et al., 2013; Botter et al., 2010). The shape of travel time distributions depends on the assumed storage selection scheme (SAS functions), which specifies the time-variance of travel times, and the preference of Q and ET to remove water of a certain age from storage (Rinaldo et al., 2015; van der Velde et al., 2012). In this study, we opted for a SAS function describing variable flow with time-varying storage selection (see section S2 in the SM). This means that travel time distributions are time-variant and different for ET, Q, and storage, and that the preference of discharge (Q) for water of a certain age depends on storage (i.e., SAS-function of discharge changes with storage in the transport zone; van der Velde et al., 2015; Harman, 2015). Travel time distributions were calculated for the modelled fluxes from the source and transport zone, which, in turn, yielded pesticide concentrations

in Q_{sz}, Q_{tz}, and E_{tz} (i.e., C_{sz}, C_{tz}, C_{ET}; Table 2). A detailed description of travel time distributions and related mixing schemes can be found in, e.g., van der Velde et al. (2012), Botter et al. (2010), and Harman (2015).

2.6 Pesticide model: mass transfer and transport

The applied pesticide enters the model system via the source zone (mass flux Φ_{inp} in Fig. 2) and is assumed to be initially
5   present in the sorbed phase of the source zone, given the physico-chemical properties of S-metolachlor. The reasoning behind this is that farmers tend to apply pesticides during dry periods, after which most of the applied water will evaporate, leaving the pesticides sorbed to soil particles or in the more tightly bound soil water. In support of this assumption, previous studies have found strong sorption of S-metolachlor to surface soils, where the organic matter content is typically higher than at greater depth (e.g. Bedmar et al., 2011; Rice et al., 2002; Si et al., 2009). Subsequently, infiltration of precipitation leads
10   to pesticide desorption and input into the dissolved phase of the source zone reservoir. Infiltration mobilizes only a fraction of the adsorbed pesticide in the source zone reservoir depending on the contact time between water and soil. Hence, pesticide concentrations in the source zone reservoir decrease with increasing water flow and thus decreasing contact time between soil matrix and infiltrating water. This mimics limited pesticide desorption and uptake in water for preferential flow (see Table 2, term $(1 - e^{-lT_{sz}})$ in the equation for $C_{sz}(t)$) and is similar to the approach used in van der Velde et al. (2010) to
15   simulate nitrate retention in the topsoil. Pesticide in the dissolved phase is exported from the source zone via discharge (Φ_{sz}), which leads to pesticide input into the transport zone (Φ_{r}) and potentially direct transport to the catchment outlet via overland flow (i.e., in the dissolved phase after desorption; Φ_{of}). The model also accounts for direct pesticide transport from the source zone to the catchment outlet in the particulate phase via eroded material (Φ_{er}; without desorption). The eroded pesticide amount was assumed proportional to discharge via overland flow and stored pesticide mass in the source zone (related by
20   model parameter f_{er}, Table 2). Hence, the erosion pathway (Φ_{er}) removes sorbed pesticide from the source zone and thus plays an important role for the overall pesticide mass balance.

Pesticide in the transport zone can be discharged to the catchment outlet (Φ_{tz}) or return to the source zone *via* evapotranspiration from the transport zone (Φ_{et}). Φ_{et} was assumed to redirect a fraction of the pesticide mass back into source zone storage (Φ_{ex}; Benettin et al., 2013; Bertuzzo et al., 2013; Queloz et al., 2015) to account for incomplete uptake
25   of pesticide in ET water by plants and pesticide release to the soil after plant uptake (Al-Khatib et al., 2002; Henderson et al., 2007). Dissolved pesticide concentrations at the catchment outlet were calculated from concentrations in overland flow (Φ_{of}) and discharge from the transport zone (Φ_{tz}). Concentrations and δ^{13}C-values of S-metolachlor were simulated in the dissolved phase at the catchment outlet (C and δ^{13}C in Fig. 2, respectively) on a daily time step. Following Bertuzzo et al. (2013), sorption in the transport zone was not considered in the model in order to limit model complexity, and in view of the
30   rapid decrease in the soil organic matter content with depth (i.e., from about 2.5 % at the surface to 0.6 % below 1 m depth). Table 2 shows the detailed equations for pesticide storage, mass fluxes and concentrations.

2.7 Pesticide model: degradation and isotope fractionation

We considered biodegradation as the main process of S-metolachlor mass reduction in the catchment (Accinelli et al., 2001; Miller et al., 1997). We simulated first-order kinetics with a constant half-life in the source zone as previously described in Bertuzzo et al. (2013) and Queloz et al. (2015). For the transport zone, we simulated an exponential decline of the degradation rate constant with travel time (see Table 2, term $e^{-\frac{r_0}{k}(1-e^{-kT}T_{tz})}$ in the equations for $C_{tz}(t)$ and $C_{ET}(t)$), which resembles a linear decrease in the degradation rate with depth given an exponential increase in travel time with depth (van der Velde et al., 2010). This mirrors slower pesticide degradation in deeper soil layers compared to the topsoil due to decreasing microbial activity (Rodríguez-Cruz et al., 2006; Si et al., 2009).

The model was applied to explicitly calculate concentrations of light and heavy carbon isotopes contained in the pesticide. This allowed for the simulation of degradation-induced isotope fractionation: the light isotopes degrade with a rate constant r_0^{12}, which is related to the rate constant of the heavy isotopes (r_0^{13}) by the isotope fractionation factor α ($\alpha < 1$) as $r_0^{13} = \alpha \cdot r_0^{12}$. Modelled δ^{13}C-values at the catchment outlet were calculated from the simulated concentrations of the light and heavy carbon isotopes following Eq. (1). For model simplicity and because of the lack of more detailed information, we assumed a single degradation mechanism with one unique fractionation factor (α). In the following, we will refer to the carbon isotopic enrichment factor $\varepsilon_C = 1 - \alpha$ (reported in ‰) instead of α.

Considering the physico-chemical properties of S-metolachlor (Table S1), we disregarded abiotic degradation processes (e.g., photolysis) and potential associated isotope fractionation effects in the modelling. We neither simulated sorption-induced isotope fractionation, which is considered insignificant during limited numbers of sorption-desorption steps (Kopinke et al., 2017). Moreover, we disregarded pesticide transfer to and from the atmosphere (i.e., volatilization and deposition), as we consider volatilization to be minor based on the relatively low Henry's Law constant of S-metolachlor and previous research on volatilization of S-metolachlor (Parochetti, 1978; Rice et al., 2002; Rivard, 2003). We assumed instead that the water in the pesticide spray is rapidly lost by evaporation, leaving the remaining pesticide adsorbed to soil. Subsequently, wind-induced erosion might lead to further redistribution of the sorbed pesticide. However, we disregarded wind-induced erosion in the modelling as this process is difficult to quantify and likely secondary in the study catchment relative to erosion via overland flow.

2.8 Input data and calibration

The model simulated discharge, pesticide concentrations and δ^{13}C-values from 1 September 2004 to 31 December 2012 to ensure sufficient model spin-up time. It was run with daily data for precipitation and potential evapotranspiration (E_{pot}) from the meteorological station Waltenheim sur Zorn. Pesticide input rates and dates of pesticide application for each simulation year were set to the application rates and dates of S-metolachlor in 2012 (obtained from the survey among the farmers). No pesticide was present in the model domain at the beginning of the simulation.

Calibration was performed for 18 model parameters (ranges of parameter values are provided in Table 3) against the following measured data: daily average of discharge at the catchment outlet (Fig. 1) between 9 March and 14 August 2012; 33 flow-proportional samples of S-metolachlor concentrations at the catchment outlet between 20 March and 21 August 2012, among which six with $\delta^{13}C$-values; and one grab sample of S-metolachlor concentrations at the catchment outlet on 20

5 November 2012. The initial $\delta^{13}C$-value of the applied S-metolachlor was specified a priori as $\delta^{13}C_0$ = -32.5 ‰ to be able to simulate $\delta^{13}C$-values as low as -32.4 ‰ measured at the catchment outlet. The $\delta^{13}C_0$-value in the model was thus more negative than the $\delta^{13}C$-value of the S-metolachlor formulation exclusively used in the plot experiment ($\delta^{13}C$ = -31.9±0.3 ‰). We did not include spatial variability in the initial $\delta^{13}C$-value of S-metolachlor due to the predominant use (about 80 %) of one commercial S-metolachlor product according to the survey among the farmers.

10 Model performance of each parameter set was calibrated using a combined objective function (N_{comb}) that simultaneously evaluates the Nash-Sutcliffe coefficients for discharge (N_Q), concentrations (N_C) and $\delta^{13}C$-values of S-metolachlor ($N_{\delta 13C}$; see section S5 in the SM for a detailed description). In view of the relatively few field data, we opted for a threshold value for N_{comb} of 0.7 (based on preliminary model calibrations) defining equally suitable (i.e., behavioural) model results similar to the GLUE approach (Beven, 2012). This criterion was used in 10,000 calibration runs to determine 10,000 behavioural

15 parameter sets with the particle swarm optimization algorithm implemented in the open-source R package "HydroPSO" (Zambrano-Bigiarini and Rojas, 2013).

3 Results and Discussion

3.1 Monitoring results: pesticide concentrations and $\delta^{13}C$-values

Concentrations of dissolved S-metolachlor in surface runoff from the plot between April and mid-July were highest during

20 the first runoff event (64.1 µg L^{-1} on 17 April; Table S2) that followed S-metolachlor application (12 April; Fig. 3c). Concentrations at the plot remained above 10 µg L^{-1} during the study period (except for 19 June), which underscores the persistence of S-metolachlor in the soil throughout summer (field-derived half-life of 54 days; Lefrancq, 2014). At the catchment outlet, S-metolachlor concentrations were below 0.1 µg L^{-1} in March and April (Fig. 3d and Table S4), which indicates negligible pesticide residues from previous years. S-metolachlor was mainly mobilized during the extreme rainfall-

25 runoff event on 21 May with maximum concentrations of 62.1 µg L^{-1} (dissolved phase) as opposed to low concentrations before. During this runoff event, concentrations at the catchment outlet were similar to concentrations at the plot on 17 April (Fig. 3c and d). In subsequent runoff events, concentrations at the catchment outlet gradually decreased from 6.1 µg L^{-1} (end of May) to around 0.1 µg L^{-1} (August). As the plot samples were exclusively fed by surface runoff, larger concentrations at the plot compared to the catchment highlight the importance of surface runoff as transport route for S-metolachlor in the

30 Alteckendorf catchment. At catchment scale, such localised surface runoff re-infiltrated before reaching the catchment outlet in the first weeks of the study period. The first occurrence of surface runoff at the catchment outlet was thus later (i.e., on 2 May), after a sealing crust on the silty soil had developed, which resulted in large areas of surface runoff close to the

catchment outlet. In addition to limited pesticide application before May, this explains the lack of concentration peaks in April, as opposed to what has been observed at the plot.

Concentrations in the grab samples from the drain outlet reached a maximum of 2.21 µg L^{-1} following the extreme rainfall event; the mean value of all samples was 0.28±0.52 µg L^{-1} (n = 16; Fig. 3e and Table S3). However, potential concentration peaks during high flow could not be captured, as the drain outlet was below the water level and thus not accessible under high-flow conditions. Nonetheless, assuming minor concentration variations outside high-flow periods, the low concentrations at the drain outlet suggest a secondary contribution to herbicide export from drain outflow and groundwater seepage.

The decreasing concentrations at the plot and catchment outlet with successive runoff events in May and June indicate a gradual depletion of the topsoil herbicide pool, which might be ascribed to herbicide transport via surface runoff, infiltration into deeper soil layers, and/or degradation between the runoff events. The occurrence of degradation is supported by the field CSIA data: δ^{13}C-values of S-metolachlor at the plot and catchment were in the range of the applied product (-31.9±0.31 ‰ in the application tank) during the first runoff events in May (-32.2 to -31.6 ‰ at the plot and -32.4 to -31.6 ‰ at the catchment outlet) and became gradually enriched in June and July, yielding an increase by 2.6 ‰ at the plot (between 22 May and 10 July; Fig. 3c and Table S2) and by 2.5 ‰ at the catchment outlet (between 21 May and 17 July; Fig. 3d and Table S4). As opposed to the concentration data, CSIA data thus give clear evidence of in situ degradation of S-metolachlor. The magnitude of isotopic enrichment indicates a similar extent of degradation at the plot and catchment scale. This suggests that degradation-induced fractionation effects primarily occurred in the topsoil, as the plot experiment only captured herbicide in surface runoff remobilized from the topsoil. Given that pesticide residues from previous years in the topsoil were secondary, this also implies that the isotopic enrichment occurred in the course of around two months.

As the first samples do not show significant enrichment (assuming the same initial δ^{13}C-value for the bulk pesticide as for the pesticide applied at the plot), degradation might have mainly occurred from June on, following a period of little degradation in April and May. This might result from the generally limited availability of sorbed pesticides for microbial degradation (e.g., Dyson et al., 2002; Guo et al., 2000; Park et al., 2003), which, in turn, hampers degradation-induced fractionation before the first rainfall event of May 21. Moreover, little degradation before June may be explained by lower soil temperature in spring (daily mean air temperatures mostly between 5 and 10°C in April and around 10°C on several days in May), resulting in lower microbial activity (Dinelli et al., 2000; Barra Caracciolo et al., 2005).

Acetochlor concentrations at the plot peaked during the first runoff event on 17 April (Fig. 3h), but at a much lower concentration (1.8 µg L^{-1}) than S-metolachlor, as acetochlor had not been applied at the plot in 2012. Its frequent detection in the plot samples must, therefore, be ascribed to contamination from surrounding fields due to atmospheric drift, wind-induced erosion, or, possibly, to applications in previous years. Acetochlor at the plot shows a pronounced isotopic enrichment between two samples from the end of May and mid-June, respectively (Fig. 3h). However, as it had not been applied at the plot, other processes than transformation might be at the origin of this enrichment.

Concentrations of acetochlor at the catchment outlet (Fig. 3i and Table S4) were comparable to those of S-metolachlor (Fig. 3d). As observed for S-metolachlor, concentrations of acetochlor at the catchment outlet were highest in response to the rainfall event on 21 May, and rapidly decreased afterwards. However, the last two samples show a concentration increase following very low concentrations in July. This could result from a second application of the compound (not suggested by the survey among the farmers), or a delayed arrival of the pesticide in the drainage network due to slow pesticide transport through the soil matrix. In contrast, concentrations of acetochlor at the drain outlet were below 1 µg L^{-1} in all samples (Fig. 3j and Table S3). Hence, this supports the assumption of a minor contribution of drain outflow and groundwater seepage to overall pesticide export.

Similar to S-metolachlor, δ^{13}C-values of acetochlor at the plot and catchment scale became significantly enriched between May and July (enrichment above 3 ‰; Fig. 3h and i, and Table S2 and S4). This confirms the hypothesis of similar isotope fractionation effects at both spatial scales and the dominant role of degradation in the topsoil compared to deeper soil layers. However, in the case of acetochlor, plot samples show a systematic shift of approximately 4 ‰ towards more depleted values compared to the catchment samples. As acetochlor was not applied at the experimental plot, it is unclear whether this shift reflects isotope fractionation effects due to, e.g., volatilization, or deposition of a more depleted acetochlor formulation used on another field.

3.2 Modelling results: multiple model calibrations

The model generally captured measured discharge at the catchment outlet (Fig. 4b). It also succeeded in reproducing the low S-metolachlor concentrations prior to pesticide application and the concentration peaks during high-flow conditions, with the maximum occurring in response to the extreme rainfall event on May 21 (Fig. 4c). The ranges of modelled concentrations and δ^{13}C-values were comparably narrow between May and August; they were much wider outside this period when model results were not constrained by calibration to samples with CSIA data and concentrations above the detection limit, respectively (Fig. 4c and d).

Although erosion and overland flow in the model were triggered several times during the study period, their impact on concentrations was minor apart from the response to the extreme rainfall event. Hence, the model underestimated peaks in discharge and concentrations (Fig. 4b and c). Some calibrations yielded concentrations in the low ng L^{-1} range in late summer due to the absence of pesticide release from the source zone (Fig. 4c). In early autumn, however, pesticide concentrations increased following precipitation and associated pesticide release. Accordingly, the model simulated persistence of S-metolachlor in topsoil throughout summer, which is in agreement with the detection of S-metolachlor at the catchment outlet even several months after the pesticide applications (e.g., concentration of 0.1 µg L^{-1} in the grab sample on 20 November 2012).

The model predicted a gradual increase in δ^{13}C-values after pesticide application in April and May. This reflects isotopic enrichment in discharge from the transport zone due to pesticide degradation. Simulated δ^{13}C-values outside the study period were associated with a wide range of possible values, and highlight a pronounced isotopic enrichment in early autumn (Fig.

11

4d). Moreover, simulated δ^{13}C-values suggest the occurrence of local minima following rainfall events. Rainfall events mobilized pools of sorbed and thus non-degraded pesticide in the source zone, which was thereby transferred to the transport zone (and secondarily to overland flow). The temporal predominance of non-degraded pesticide pools in discharge led, in turn, to relatively low δ^{13}C-values at the catchment outlet. In addition, rainfall events resulted in temporally decreasing travel times, which limited reaction time and thus isotope fractionation in the transport zone. The minima in δ^{13}C-values were most distinct after the second S-metolachlor application at the plot (May 1), and after the extreme rainfall event on May 21 (Fig. 4d); they were much less pronounced in late autumn and winter, when most of the pesticide had already been removed from the source zone. Due to the limited temporal resolution of the field CSIA data, it is not possible to conclude whether these fluctuations occurred in reality. However, because of these model results, it becomes apparent that CSIA measurements both before and after rainfall events are particularly valuable to understand the extent of remobilization of sorbed pesticides from the source zone.

Before the first minimum in δ^{13}C-values on May 1, the increase in δ^{13}C-values levelled off in most calibration runs, attaining an upper limit of isotopic enrichment. The pesticide reaching the catchment outlet before May is associated with long travel times, which results in a significant decrease in the rate of pesticide degradation in the transport zone (exponential decrease with travel time) and thus inhibits further isotope fractionation. As with the minima in δ^{13}C-values following rainfall events, it would be beneficial to compare these model results with field CSIA data. However, as CSIA cannot currently be performed at such low pesticide concentrations without interferences, measurements during these time periods might, for now, not provide additional information on pesticide fate.

The calibration results yielded a smaller half-life in the source zone (mean = 5.6 d; range from 5.1 d to 14.7 d) than reported half-lives for S-metolachlor (15 - 54 d; Table S1). In contrast, half-lives in the transport zone were considerably larger due to decelerated degradation with longer travel times (i.e., increasing depth). For example, averaged over all simulations, model half-lives in the transport zone were 63.9 d and 2310.2 d at depths corresponding to travel times of six months and one year, respectively. This yielded the simulated long tailing of S-metolachlor concentrations in discharge from the transport zone (Fig. 4c).

The Nash-Sutcliffe efficiency of the 10,000 simulation results ranged from $N_{comb} = 0.7$ to $N_{comb} = 0.92$ (mean of 0.88). Overall, the model shows good parameter identifiability for most parameters (i.e., clear maxima in parameter histograms; Fig. S1). The only parameters with a limited identifiability in the flow model are those defining the SAS functions for ET (α_{ET}) and old water in discharge from the transport zone (β_Q), respectively. The pesticide model shows a limited identifiability for the parameter determining pesticide transport in ET from the transport zone to the source zone (f_{ex}), as well as for the calibration factor of the applied pesticide mass (m_{IN}). Hence, based on the measured data, it was not possible to distinguish the effects of ET and old water discharge on pesticide concentrations in the study catchment. Nonetheless, these two processes are important for pesticide retention in the catchment and the time lag between pesticide application and release to streamwater.

3.3 Modelling results: quantification of pesticide transport and degradation

The model allows tracking pesticide transport and degradation in all compartments of the simulated system (Table 4 and Fig. 5). The mean pesticide export from the catchment based on 10,000 simulations was 4.6±5.3 % of the applied mass in the study period and 4.7±5.3 % in the entire year 2012, of which the majority occurred via erosion (i.e., 3.8±5.2 % of the total mass in both time frames). The minor difference in pesticide export between the two time frames underlines the importance of the extreme rainfall event, which entailed more than 99 % of the overall pesticide transport via erosion in 2012 (see jump in mass balance term in Fig. 5f). Discharge from the transport zone accounted for the remaining 0.3 % and 0.4 % in the study period and 2012, respectively, which is in line with low concentrations at the drain outlet (Fig. 3e). The average extent of pesticide degradation in 2012 was 92.6±5.9 % of the applied mass. With 80.8±6.5 % of total degradation occurring in the source zone and 11.8±5.0 % in the transport zone, respectively, the source zone accounted for the majority of pesticide degradation in the catchment (Fig. 5e).

The differing mass balance terms for pesticide transport between 2011 and 2012 highlight the importance of erosion for simulated pesticide export from the catchment. Erosion accounted for the bulk of pesticide transport in 2012 albeit with large variations among individual model runs (Fig. 5f), whereas it barely occurred in the simulation of 2011 (Table 4). Similarly, pesticide export via the transport zone in 2011 was minor with a proportion of 0.1 % of the total applied pesticide mass. Therefore, pesticide retention in the catchment was larger at the end of 2011 (4.4±2.5 %) compared to 2012 (2.7±2.0 %).

3.4 Insights on pesticide fate and transport from the model

The model allowed for testing alternative representations of pesticide transport and degradation. We set up three modified models and calibrated each in 1000 simulations against the same data as the original model presented before. First, 1000 simulations were run without pesticide degradation and calibrated against measured discharge and concentrations. Concentrations remained above 10 μg L^{-1} during most of the year and the observed concentration decline from May to September could not be reproduced even with increased erosion (Fig. S2). Hence, this illustrates the need for simulating pesticide degradation in the model. Second, the original model was applied without pesticide transport via erosion (but overland flow was kept) and calibrated against discharge, concentrations and δ^{13}C-values. The lack of mass loss via erosion was counterbalanced by increased degradation in the transport zone. In contrast, degradation in the source zone decreased, on average, relative to the original model, which resulted in comparable isotopic enrichment factors with the two model setups (i.e., mean of ε_C = -1.0±0.4 ‰ vs. ε_C = -0.9±0.3 ‰ in the original model). Overall, the simulation results of the model without erosion are similar to those of the original model (Fig. 6a). However, the behavioural simulations of the model with erosion (i.e., original model) yielded a smaller range of concentrations and δ^{13}C-values outside the calibration period than the model without erosion. This suggests that including erosion, as done in the original model, improves the model representation of pesticide transport.

13

The third modification consisted in a model with erosion and degradation, with the latter being implemented by a constant degradation half-life in both the source and transport zones instead of a declining first-order degradation rate constant with increasing travel time in the transport zone (cf. equation for $C_{tz}(t)$ in Table 2). This model was again calibrated against measured discharge, concentrations, and δ^{13}C-values. Differences between the original and the modified model with a constant degradation half-life (Fig. 6b) were even more distinct than for the model without erosion (Fig. 6a). Again, much smaller simulated ranges of concentrations and δ^{13}C-values outside the study period demonstrate the model improvement with a declining degradation rate constant with increasing travel time (as implemented in the original model). The decrease in Nash-Sutcliffe efficiency of simulated concentrations (N_C, Eq. S6) for the model with a constant degradation half-life is comparable to the decrease in Nash-Sutcliffe efficiency for the model without erosion (i.e., $N_C = 0.83$ in the original model vs. $N_C = 0.74$ with a constant degradation half-life and $N_C = 0.73$ without erosion).

For the modified model with a constant degradation half-life, degradation in the transport zone was faster compared to the original model, which led to substantially lower concentrations than the measured values (note the log-scaling in (Fig. 6b, iii)) and more enriched δ^{13}C-values in autumn and spring (i.e., when the majority of the pesticide is in the transport zone) compared to the original model. The extent of degradation in the source zone was, on the contrary, smaller than in the original model, which resulted in slightly less overall degradation in the model with a constant degradation half-life (i.e., mean of 90.8 % vs. 92.6 % in the original model). Consequently, with a mean of $\varepsilon_C = -1.3\pm0.7$ ‰, the calibrated enrichment factor was slightly larger than with the original model (i.e., $\varepsilon_C = -0.9\pm0.3$ ‰).

Whereas previous pesticide fate studies have frequently assumed a constant degradation half-life for pesticides over the entire subsurface depth (e.g., Fohrer et al., 2014; Gassmann et al., 2014; Pullan et al., 2016; Wittmer et al., 2016), the comparison between the original model and the modified model (with a constant half-life) supports the simulation of an increasing half-life with increasing subsurface depth. This can be easily implemented in our model by means of travel-time distributions. In summary, none of the alternative model setups resulted in better model fits or smaller uncertainties such that the original model was considered most appropriate for simulation of pesticide transport and degradation in the study catchment.

The model results suggest that persistence of S-metolachlor in the environment is strongly coupled to pesticide sorption in the source zone. By assuming no decay of sorbed pesticides in the source zone and desorption of pesticides during rainfall events, we were able to describe the observed long persistence and relatively small increase in δ^{13}C-values with time. In our conceptual model, each rainfall event mobilizes a part of the non-decayed sorbed pesticide, which effectively lowers the δ^{13}C-value of the mobile soil water after each rainfall event. The pesticide concentration of pulses with low δ^{13}C-value decline with increasing time after application as most of the sorbed pesticides has been transported out of the source zone (cf. section 3.2). Based on these results, but out of reach for our study, further investigations are needed to check for the occurrence of such episodes of declining δ^{13}C-values after rainfall events long after pesticide application in order to support our model concepts.

In addition to testing of different model setups, we used our conceptual model to assess a field-integrated enrichment factor (ε_C). We propose that travel-time distribution modelling inherently accounts for dispersion and flowpath mixing (Hrachowitz et al., 2016) and is thus able to mirror attenuation of potentially large isotope fractionation due to dispersion and mixing in open systems (Abe and Hunkeler, 2006; Lutz et al., 2013; van Breukelen and Prommer, 2008). In contrast, enrichment factors derived from field CSIA data via the Rayleigh equation (Eq. S2) are prone to underestimate the "true" enrichment factor in open systems (Abe and Hunkeler, 2006; van Breukelen, 2007). Hence, conceptual travel-time based models represent an alternative way of assessing field-integrated enrichment factors, which might improve in accuracy with increased temporal resolution of CSIA samples. With a mean ε_C of -0.9±0.3 ‰ and a best-fit value of -1.13 ‰ in this study, the calibrated ε_C for S-metolachlor is smaller (i.e., corresponding to less fractionation) than experimentally determined ε_C-values for the chloroacetanilides alachlor (ε_C = -2.0±0.3 ‰) and acetochlor (ε_C = -3.4±0.5 ‰; Elsayed et al., 2014). This is also the case for the two alternative model setups discussed above (i.e., mean values of ε_C = -1.3±0.7 ‰ with a constant degradation half-life and ε_C = -1.0±0.4 ‰ without erosion, respectively). However, enrichment factors may differ between compounds of the same pesticide group and even between microbial degradation pathways of the same compound (Hartenbach et al., 2008; Meyer and Elsner, 2013; Meyer et al., 2009; Penning et al., 2010; Penning and Elsner, 2007).

3.5 Degradation assessment with the Rayleigh equation and the model

Previous modelling studies have demonstrated that the Rayleigh equation (Eq. S2) systematically underestimates the actual extent of degradation (Abe and Hunkeler, 2006; van Breukelen and Prommer, 2008; van Breukelen and Rolle, 2012; Lutz et al., 2013). The underestimation by the Rayleigh equation results from attenuation of effective isotope fractionation by dispersion and mixing processes in real-world flow systems, which is disregarded in the Rayleigh equation. In this study, we compared the extent of degradation known from the simulated concentrations and the model mass-balance, respectively, with the one estimated by the Rayleigh equation. This enables us to assess the reliability of the Rayleigh equation to estimate degradation at catchment scale. We made use of simulated (virtual) CSIA data to assure unbiased comparison of continuous time-series.

Assuming the same enrichment factor and initial isotopic signature of the applied product as in the best-fit simulation (i.e., ε_C = -1.13 ‰ and $\delta^{13}C_0$ = -32.5 ‰, respectively), the Rayleigh equation approach gave an extent of degradation of $D_{Rayleigh}$ = 94.1 % (Eq. S3) for the simulated $\delta^{13}C$-value of -29.4 ‰ on 17 July (i.e., best-fit simulation on last day of field CSIA data). In comparison, based on the simulated concentrations of S-metolachlor and a conservative tracer at the catchment outlet (for the entire simulation period from 2004 to 2012), the actual extent of degradation on 17 July was D_{Sample} = 99.9 % (Eq. S4) in the best-fit simulation. Overall, the Rayleigh equation applied to (virtual) CSIA data from the catchment outlet underestimated the actual extent of degradation as occurred for the outlet sample (i.e., $D_{Rayleigh} < D_{Sample}$; Fig. 7e) in agreement with earlier studies (see above). In this study, the underestimation of D_{Sample} was more pronounced during high flow periods (soon after pesticide application) compared to baseflow periods (Fig. 7), which is in agreement with Lutz et al.

(2013). High flow periods in the model were associated with input of barely degraded pesticide, which, therefore, masked significant isotope fractionation in pesticide from the transport zone.

Employing the best-fit estimate of ε_C = -1.13 ‰, $D_{Rayleigh}$ was always larger than the actual extent of degradation in the entire catchment derived from the mass balance of the model in 2012 ($D_{Catchment}$; Fig. 7e). For example, $D_{Catchment}$ was 72.9 % on 17 July, which is considerably smaller than the Rayleigh estimate for the outlet sample ($D_{Rayleigh}$ = 94.1 %; both for the best-fit simulation). In contrast to $D_{Rayleigh}$ versus D_{Sample}, the deviation between $D_{Rayleigh}$ and $D_{Catchment}$ was largest during baseflow periods (with relative deviations of more than 50 % during the study period), and sharply decreased for high flow conditions (Fig. 7). This can be explained by the large extent of degradation for pesticide in slow discharge from the transport zone during baseflow, which is not representative of the overall extent of degradation in the catchment, as opposed to discharge of less-degraded pesticide during high flow conditions (associated with recent desorption and short travel times). Accordingly, as most of the pesticide was contained in the source zone reservoir especially shortly after pesticide application, $D_{Rayleigh}$ was closer to $D_{Catchment}$ for samples with a dominant imprint of the source zone (i.e., during high flows). This suggests that CSIA-based degradation estimates are most representative of catchment-scale decay for samples taken during high flow conditions, when pesticide discharge occurs via shallow soils mainly. This result further emphasizes the need for studies on topsoil sorption and desorption of S-metolachlor under field conditions and realistic application scenarios.

Laboratory-derived carbon enrichment factors of pesticides are subject to uncertainty ranges typically between ±0.1 ‰ and ±1.0 ‰ (Elsayed et al., 2014; Meyer and Elsner, 2013; Wu et al., 2014). In order to assess the uncertainty in Rayleigh equation estimates, we considered an uncertainty range of ±0.5 ‰ for ε_C around the best-fit value (i.e., -1.63 ‰ $\leq \varepsilon_C \leq$ -0.63 ‰) and assumed that the simulated δ^{13}C-values of the best-fit calibration describe the actual δ^{13}C-values. The Rayleigh equation yielded the largest uncertainty range in degradation estimates in response to rainfall events (green area in Fig. 7e). For example, whereas the best-fit estimate with ε_C = -1.13 ‰ gave $D_{Rayleigh}$ = 94.1 % on July 17, $D_{Rayleigh}$ ranged between 85.9 and 99.4 % on that day with ε_C = -1.13±0.5 ‰. Nonetheless, the mean absolute deviation from the best-fit simulation was below 3.5 % in 2012 (maximum deviation of 21.1%). Hence, despite an uncertainty range of ±0.5 ‰ in ε_C, the Rayleigh equation estimate remained within an acceptable error band and thus allowed for a first (conservative) approximation of the extent of degradation at the catchment outlet.

Overall, these results suggest that CSIA data and CSIA-based (i.e., Rayleigh-equation based) estimates are not representative for the entire catchment. Hence, the modelling approach is required in order to upscale CSIA information on degradation to the catchment scale, which is crucial in the quantification of pesticide residues in the catchment.

4 Conclusions

This study presents the first measurements of herbicide CSIA-data at catchment scale. Carbon isotope ratios of the herbicides S-metolachlor and acetochlor at the catchment outlet indicated a delayed onset of pesticide degradation after a period of little degradation during spring. S-metolachlor degradation and transport was simulated in a conceptual (i.e., parsimonious

mathematical) hydrological model based on travel time distributions. The simulation results underlined that assessment of pesticide degradation at catchment scale with a constant half-life (e.g., derived from topsoil studies) might lead to overestimation of pesticide degradation in deeper soil layers and thus overly optimistic expectations on environmental protection. In addition, the model results demonstrated that degradation estimates via the Rayleigh equation are considerably larger than the overall extent of degradation within the catchment (calculated from the model mass-balance). This implies that a large isotopic enrichment of streamwater samples does not necessarily correspond to a large extent of pesticide degradation in the entire catchment, as it can also result from transient contributions of flowpaths associated with more pronounced degradation relative to the bulk of the pesticide mass. Moreover, laboratory-derived enrichment factors might not be suitable for degradation assessment with the Rayleigh equation at catchment scale, provided that such values are available for the examined compound at all. Hence, conceptual modelling based on travel time distributions can prove beneficial as complementary approach in the evaluation of pesticide degradation for streamwater samples and the entire catchment.

The model indicated that the dynamics of CSIA data at the catchment outlet were highly responsive to changing hydrological conditions (e.g., following rainfall events). As CSIA measurements in this study were only possible after rainfall-events and not during low-flow periods, we were not able to corroborate this model result. This implies that additional CSIA data at higher temporal resolution (ideally at the same resolution as concentration data) and at later times of the study period especially during low flow conditions can yield a much clearer picture of pesticide transport and degradation. Such data might further improve the representation of pesticide degradation in models building on the conceptual model presented in this paper, and allow for the use of CSIA data as tracer for different flowpaths at catchment scale.

Depending on the study-compound properties, future modelling studies might include additional processes such as re-equilibration between pesticide in the dissolved and particulate phase. Similarly, incorporation of sorption processes in the transport zone would be an important future step with this model setup, as sorption might still occur in deeper soil despite decreasing organic matter content with depth. Nonetheless, insights from this study highlight how conceptual modelling of pesticide degradation and transport with travel-time distributions can advance our understanding of pesticide fate and contribution of different transport pathways at catchment scale, and pinpoint knowledge gaps for which additional measurements are required, especially when applied in a combined experimental and modelling approach. As travel-time based models are computationally non-intensive and can be applied in the absence of spatially distributed information on parameters (e.g., soil hydraulic properties), they can also be useful for the implementation of monitoring and regulation tests in agricultural catchments.

Data availability

The measured data can be found in the supplement to this article (section S3).

Competing interests

The authors declare that they have no conflict of interest.

References

Abe, Y.; Hunkeler, D., Does the Rayleigh equation apply to evaluate field isotope data in contaminant hydrogeology? Environ. Sci. Technol. 2006, 40, (5), 1588-1596, doi:10.1021/es051128p.

Accinelli, C.; Dinelli, G.; Vicari, A.; Catizone, P., Atrazine and metolachlor degradation in subsoils. Biol Fertil Soils 2001, 33, (6), 495-500, doi: 10.1007/s003740100358.

Al-Khatib, K.; Baumgartner Unland, J.; Olson, B. L. S.; Graham, D. W., Alachlor and metolachlor transformation pattern in corn and soil. Weed Science 2002, 50, (5), 581-586, doi:10.1614/0043-1745(2002)050[0581:AAMTPI]2.0.CO;2.

Atteia, O.; Franceschi, M.; Dupuy, A., Validation of reactive model assumptions with isotope data: Application to the Dover case. Environ. Sci. Technol. 2008, 42, (9), 3289-3295, doi:10.1021/es071269m.

Barra Caracciolo, A.; Giuliano, G.; Grenni, P.; Guzzella, L.; Pozzoni, F.; Bottoni, P.; Fava, L.; Crobe, A.; Orrù, M.; Funari, E., Degradation and leaching of the herbicides metolachlor and diuron: a case study in an area of Northern Italy. Environmental Pollution 2005, 134, (3), 525-534, doi:10.1016/j.envpol.2004.08.014.

Battaglin, W. A.; Goolsby, D. A., Are Shifts in Herbicide Use Reflected in Concentration Changes in Midwestern Rivers? Environ. Sci. Technol. 1999, 33, (17), 2917-2925, doi:10.1021/es9900149.

Bedmar, F.; Daniel, P. E.; Costa, J. L.; Giménez, D., Sorption of acetochlor, S-metolachlor, and atrazine in surface and subsurface soil horizons of Argentina. Environmental Toxicology and Chemistry 2011, 30, (9), 1990-1996, doi:10.1002/etc.602.

Benettin, P.; van der Velde, Y.; van der Zee, S. E. A. T. M.; Rinaldo, A.; Botter, G., Chloride circulation in a lowland catchment and the formulation of transport by travel time distributions. Water Resour. Res. 2013, 49, (8), 4619-4632, doi:10.1002/wrcr.20309.

Bertuzzo, E.; Thomet, M.; Botter, G.; Rinaldo, A., Catchment-scale herbicides transport: Theory and application. Advances in Water Resources 2013, 52, (0), 232-242, doi:10.1016/j.advwatres.2012.11.007.

Beven, K., Parameter Estimation and Predictive Uncertainty. In Rainfall-Runoff Modelling, John Wiley & Sons, Ltd: 2012; 231-287, doi:10.1002/9781119951001.ch7.

Blum, P.; Hunkeler, D.; Weede, M.; Beyer, C.; Grathwohl, P.; Morasch, B., Quantification of biodegradation for o-xylene and naphthalene using first order decay models, Michaelis-Menten kinetics and stable carbon isotopes. Journal of Contaminant Hydrology 2009, 105, (3-4), 118-130, doi:10.1016/j.jconhyd.2008.11.009.

Botter, G.; Bertuzzo, E.; Rinaldo, A., Transport in the hydrologic response: Travel time distributions, soil moisture dynamics, and the old water paradox. Water Resour. Res. 2010, 46, (3), W03514, doi:10.1029/2009WR008371.

Botter, G.; Bertuzzo, E.; Rinaldo, A., Catchment residence and travel time distributions: The master equation. Geophysical Research Letters 2011, 38, (11), L11403, doi:10.1029/2011GL047666.

D'Affonseca, F. M.; Prommer, H.; Finkel, M.; Blum, P.; Grathwohl, P., Modeling the long-term and transient evolution of biogeochemical and isotopic signatures in coal tar-contaminated aquifers. Water Resour. Res. 2011, 47, (5), W05518, doi:10.1029/2010WR009108.

Dinelli, G.; Accinelli, C.; Vicari, A.; Catizone, P., Comparison of the Persistence of Atrazine and Metolachlor under Field and Laboratory Conditions. Journal of Agricultural and Food Chemistry 2000, 48, (7), 3037-3043, doi:10.1021/jf991057b.

Divers, M. T.; Elliott, E. M.; Bain, D. J., Quantification of Nitrate Sources to an Urban Stream Using Dual Nitrate Isotopes. Environ. Sci. Technol. 2014, doi:10.1021/es404880j.

Dyson, J. S.; Beulke, S.; Brown, C. D.; Lane, M. C. G., Adsorption and Degradation of the Weak Acid Mesotrione in Soil and Environmental Fate Implications. Journal of Environmental Quality 2002, 31, (2), 613-618, doi:10.2134/jeq2002.6130.

Eckert, D.; Qiu, S.; Elsner, M.; Cirpka, O. A., Model Complexity Needed for Quantitative Analysis of High Resolution Isotope and Concentration Data from a Toluene-Pulse Experiment. Environ. Sci. Technol. 2013, 47, (13), 6900-6907, doi:10.1021/es304879d.

Elsayed, O. F.; Maillard, E.; Vuilleumier, S.; Nijenhuis, I.; Richnow, H. H.; Imfeld, G., Using compound-specific isotope analysis to assess the degradation of chloroacetanilide herbicides in lab-scale wetlands. Chemosphere 2014, 99, (0), 89-95, doi:10.1016/j.chemosphere.2013.10.027.

Elsner, M., Stable isotope fractionation to investigate natural transformation mechanisms of organic contaminants: principles, prospects and limitations. J. Environ. Monit. 2010, 12, (11), 2005-2031, doi:10.1039/C0EM00277A.

Elsner, M.; Imfeld, G., Compound-specific isotope analysis (CSIA) of micropollutants in the environment — current developments and future challenges. Current Opinion in Biotechnology 2016, 41, 60-72, doi:10.1016/j.copbio.2016.04.014.

Elsner, M.; Jochmann, M.; Hofstetter, T.; Hunkeler, D.; Bernstein, A.; Schmidt, T.; Schimmelmann, A., Current challenges in compound-specific stable isotope analysis of environmental organic contaminants. Anal Bioanal Chem 2012, 403, (9), 2471-2491, doi:10.1007/s00216-011-5683-y.

Fenner, K.; Canonica, S.; Wackett, L. P.; Elsner, M., Evaluating Pesticide Degradation in the Environment: Blind Spots and Emerging Opportunities. Science 2013, 341, (6147), 752-758, doi:10.1126/science.1236281.

Fohrer, N.; Dietrich, A.; Kolychalow, O.; Ulrich, U., Assessment of the Environmental Fate of the Herbicides Flufenacet and Metazachlor with the SWAT Model. Journal of Environmental Quality 2014, 43, (1), 75-85.

Gassmann, M.; Khodorkovsky, M.; Friedler, E.; Dubowski, Y.; Olsson, O., Uncertainty in the river export modelling of pesticides and transformation products. Environmental Modelling & Software 2014, 51, 35-44.

Grube, A.; Donaldson, D.; Kiely, T.; Wu, L. Pesticides Industry Sales and Usage 2006 and 2007 Market Estimates; U.S. Environmental Protection Agency: Washington, 2011.

Guo, L.; Jury, W. A.; Wagenet, R. J.; Flury, M., Dependence of pesticide degradation on sorption: nonequilibrium model and application to soil reactors. Journal of Contaminant Hydrology 2000, 43, (1), 45-62, doi: 10.1016/S0169-7722(99)00097-2.

Harman, C. J., Time-variable transit time distributions and transport: Theory and application to storage-dependent transport of chloride in a watershed. Water Resour. Res. 2015, 51, (1), 1-30, doi:10.1002/2014WR015707.

Hartenbach, A. E.; Hofstetter, T. B.; Tentscher, P. R.; Canonica, S.; Berg, M.; Schwarzenbach, R. P., Carbon, Hydrogen, and Nitrogen Isotope Fractionation During Light-Induced Transformations of Atrazine. Environ. Sci. Technol. 2008, 42, (21), 7751-7756, doi:10.1021/es800356h.

Henderson, K. L.; Belden, J. B.; Coats, J. R., Mass Balance of Metolachlor in a Grassed Phytoremediation System. Environ. Sci. Technol. 2007, 41, (11), 4084-4089, doi:10.1021/es061691n.

Hrachowitz, M.; Fovet, O.; Ruiz, L.; Savenije, H. H. G., Transit time distributions, legacy contamination and variability in biogeochemical 1/fα scaling: how are hydrological response dynamics linked to water quality at the catchment scale? Hydrological Processes 2015, 29, (25), 5241-5256.

Hrachowitz, M.; Benettin, P.; van Breukelen, B. M.; Fovet, O.; Howden, N. J. K.; Ruiz, L.; van der Velde, Y.; Wade, A. J., Transit times—the link between hydrology and water quality at the catchment scale. Wiley Interdisciplinary Reviews: Water 2016, 3, (5), 629-657, doi:10.1002/wat2.1155.

Hunkeler, D.; Aravena, R.; Berry-Spark, K.; Cox, E., Assessment of Degradation Pathways in an Aquifer with Mixed Chlorinated Hydrocarbon Contamination Using Stable Isotope Analysis. Environ. Sci. Technol. 2005, 39, (16), 5975-5981, doi:10.1021/es048464a.

Johannsen, A.; Dähnke, K.; Emeis, K., Isotopic composition of nitrate in five German rivers discharging into the North Sea. Organic Geochemistry 2008, 39, (12), 1678-1689, doi:10.1016/j.orggeochem.2008.03.004.

Kellman, L. M.; Hillaire-Marcel, C., Evaluation of nitrogen isotopes as indicators of nitrate contamination sources in an agricultural watershed. Agriculture, Ecosystems & Environment 2003, 95, (1), 87-102, doi:10.1016/S0167-8809(02)00168-8.

Kirchner, J. W., Catchments as simple dynamical systems: Catchment characterization, rainfall-runoff modeling, and doing hydrology backward. Water Resour. Res. 2009, 45, (2), W02429, doi:10.1029/2008WR006912.

Kopinke, F. D.; Georgi, A.; Imfeld, G.; Richnow, H. H., Isotope fractionation of benzene during partitioning – Revisited. Chemosphere 2017, 168, 508-513, doi:10.1016/j.chemosphere.2016.11.029.

Lefrancq, M. Transport and attenuation of pesticides in runoff from agricultural headwater catchments: from field characterisation to modelling. PhD thesis, Université de Strasbourg, Strasbourg, 2014.

Lefrancq, M.; Van Dijk, P.; Jetten, V.; Schwob, M.; Payraudeau, S., Improving runoff prediction using agronomical information in a cropped, loess covered catchment. Hydrological Processes 2017, 31, (6), 1408-1423, doi:10.1002/hyp.11115.

Lutz, S. R.; van Meerveld, H. J.; Waterloo, M. J.; Broers, H. P.; van Breukelen, B. M., A model-based assessment of the potential use of compound-specific stable isotope analysis in river monitoring of diffuse pesticide pollution. Hydrol. Earth Syst. Sci. 2013, 17, (11), 4505-4524, doi:10.5194/hess-17-4505-2013.

Mariotti, A.; Germon, J. C.; Hubert, P.; Kaiser, P.; Letolle, R.; Tardieux, A.; Tardieux, P., Experimental determination of nitrogen kinetic isotope fractionation: Some principles; illustration for the denitrification and nitrification processes. Plant Soil 1981, 62, (3), 413−430, doi: 10.1007/BF02374138.

Meyer, A. H.; Elsner, M., 13C/12C and 15N/14N Isotope Analysis To Characterize Degradation of Atrazine: Evidence from Parent and Daughter Compound Values. Environ. Sci. Technol. 2013, 47, (13), 6884-6891, doi:10.1021/es305242q.

Meyer, A. H.; Penning, H.; Elsner, M., C and N Isotope Fractionation Suggests Similar Mechanisms of Microbial Atrazine Transformation Despite Involvement of Different Enzymes (AtzA and TrzN). Environ. Sci. Technol. 2009, 43, (21), 8079-8085, doi:10.1021/es9013618.

Miller, J. L.; Wollum, A. G.; Weber, J. B., Degradation of Carbon-14-Atrazine and Carbon-14-Metolachlor in Soil from Four Depths. Journal of Environmental Quality 1997, 26, (3), 633-638, doi:10.2134/jeq1997.00472425002600030007x.

Milosevic, N.; Qiu, S.; Elsner, M.; Einsiedl, F.; Maier, M. P.; Bensch, H. K. V.; Albrechtsen, H. J.; Bjerg, P. L., Combined isotope and enantiomer analysis to assess the fate of phenoxy acids in a heterogeneous geologic setting at an old landfill. Water Research 2013, 47, (2), 637-649, doi:10.1016/j.watres.2012.10.029.

Park, J.-H.; Feng, Y.; Ji, P.; Voice, T. C.; Boyd, S. A., Assessment of Bioavailability of Soil-Sorbed Atrazine. Applied and Environmental Microbiology 2003, 69, (6), 3288-3298, doi: 10.1128/AEM.69.6.3288-3298.2003.

Parochetti, J. V., Photodecomposition, volatility and leaching of atrazine, simazine, alachlor and metolachlor from soil and plant material. In Meeting Weed Science Society of America: 8, Champaign, Illinois, 1978.

Penning, H.; Elsner, M., Intramolecular Carbon and Nitrogen Isotope Analysis by Quantitative Dry Fragmentation of the Phenylurea Herbicide Isoproturon in a Combined Injector/Capillary Reactor Prior to GC Separation. Analytical Chemistry 2007, 79, (21), 8399-8405, doi: 10.1021/ac071420a.

Penning, H.; Sorensen, S. R.; Meyer, A. H.; Aamand, J.; Elsner, M., C, N, and H isotope fractionation of the herbicide isoproturon reflects different microbial transformation pathways. Environ. Sci. Technol. 2010, 44, (7), 2372-8, doi:10.1021/es9031858.

Pooley, K. E.; Blessing, M.; Schmidt, T. C.; Haderlein, S. B.; Macquarrie, K. T. B.; Prommer, H., Aerobic Biodegradation of Chlorinated Ethenes in a Fractured Bedrock Aquifer: Quantitative Assessment by Compound-Specific Isotope Analysis (CSIA) and Reactive Transport Modeling. Environ. Sci. Technol. 2009, 43, (19), 7458-7464, doi:10.1021/es900658n.

Prommer, H.; Anneser, B.; Rolle, M.; Einsiedl, F.; Griebler, C., Biogeochemical and Isotopic Gradients in a BTEX/PAH Contaminant Plume: Model-Based Interpretation of a High-Resolution Field Data Set. Environ. Sci. Technol. 2009, 43, (21), 8206-8212, doi:10.1021/es901142a.

Pullan, S. P.; Whelan, M. J.; Rettino, J.; Filby, K.; Eyre, S.; Holman, I. P., Development and application of a catchment scale pesticide fate and transport model for use in drinking water risk assessment. Science of The Total Environment 2016, 563–564, 434-447, doi:10.1016/j.scitotenv.2016.04.135.

Queloz, P.; Carraro, L.; Benettin, P.; Botter, G.; Rinaldo, A.; Bertuzzo, E., Transport of fluorobenzoate tracers in a vegetated hydrologic control volume: 2. Theoretical inferences and modeling. Water Resour. Res. 2015, 51, (4), 2793-2806, doi:10.1002/2014WR016508.

Rayleigh, L. Theoretical considerations respecting the separation of gases by diffusion and similar processes. Philosophical Magazine Series 5 1896, 42, (259), 493-498, doi: 10.1080/14786449608620944.

Reinnicke, S.; Simonsen, A.; Sørensen, S. R.; Aamand, J.; Elsner, M., C and N Isotope Fractionation during Biodegradation of the Pesticide Metabolite 2,6-Dichlorobenzamide (BAM): Potential for Environmental Assessments. Environ. Sci. Technol. 2011, 46, (3), 1447-1454, doi:10.1021/es203660g.

Rice, P. J.; Anderson, T. A.; Coats, J. R., Degradation and persistence of metolachlor in soil: Effects of concentration, soil moisture, soil depth, and sterilization. Environmental Toxicology and Chemistry 2002, 21, (12), 2640-2648, doi: 10.1002/etc.5620211216.

Rinaldo, A.; Benettin, P.; Harman, C.; Hrachowitz, M.; McGuire, K.; van der Velde, Y.; Bertuzzo, E.; Botter, G., Storage selection functions: A coherent framework for quantifying how catchments store and release water and solutes. Water Resour. Res. 2015, 51, (6), 1944-7973, doi:10.1002/2015WR017273.

Rivard, L., Environmental Fate of Metolachlor. Environmental Monitoring Branch, Department of Pesticide Regulation. Sacramento, CA, 2003.

Rodríguez-Cruz, M. S.; Jones, J. E.; Bending, G. D., Field-scale study of the variability in pesticide biodegradation with soil depth and its relationship with soil characteristics. Soil Biology and Biochemistry 2006, 38, (9), 2910-2918, doi:10.1016/j.soilbio.2006.04.051.

Schmidt, T. C.; Jochmann, M. A., Origin and Fate of Organic Compounds in Water: Characterization by Compound-Specific Stable Isotope Analysis. Annual Review of Analytical Chemistry 2012, 5, (1), 133-155, doi:10.1146/annurev-anchem-062011-143143.

5   Schreglmann, K.; Hoeche, M.; Steinbeiss, S.; Reinnicke, S.; Elsner, M., Carbon and nitrogen isotope analysis of atrazine and desethylatrazine at sub-microgram per liter concentrations in groundwater. Anal Bioanal Chem 2013, 405, (9), 2857-2867, doi: 10.1007/s00216-012-6616-0.

Si, Y.; Takagi, K.; Iwasaki, A.; Zhou, D., Adsorption, desorption and dissipation of metolachlor in surface and subsurface soils. Pest Management Science 2009, 65, (9), 956-962, doi:10.1002/ps.1779.

van Breukelen, B. M., Quantifying the degradation and dilution contribution to natural attenuation of contaminants by means
10   of an open system Rayleigh equation. Environ. Sci. Technol. 2007, 41, (14), 4980-4985, doi:10.1021/es062846u.

van Breukelen, B. M.; Prommer, H., Beyond the Rayleigh equation: Reactive transport modeling of isotope fractionation effects to improve quantification of biodegradation. Environ. Sci. Technol. 2008, 42, (7), 2457-2463, doi:10.1021/es071981j.

van Breukelen, B. M.; Rolle, M., Transverse Hydrodynamic Dispersion Effects on Isotope Signals in Groundwater Chlorinated Solvents' Plumes. Environ. Sci. Technol. 2012, 46, (14), 7700-7708, doi:10.1021/es301058z.

15   van Breukelen, B. M.; Hunkeler, D.; Volkering, F., Quantification of sequential chlorinated ethene degradation by use of a reactive transport model incorporating isotope fractionation. Environ. Sci. Technol. 2005, 39, (11), 4189-4197, doi:10.1021/es048973c.

van der Velde, Y.; de Rooij, G. H.; Rozemeijer, J. C.; van Geer, F. C.; Broers, H. P., Nitrate response of a lowland catchment: On the relation between stream concentration and travel time distribution dynamics. Water Resour. Res. 2010,
20   46, (11), W11534, doi:10.1029/2010WR009105.

van der Velde, Y.; Torfs, P. J. J. F.; van der Zee, S. E. A. T. M.; Uijlenhoet, R., Quantifying catchment-scale mixing and its effect on time-varying travel time distributions. Water Resour. Res. 2012, 48, (6), W06536, doi:10.1029/2011WR011310.

van der Velde, Y.; Heidbüchel, I.; Lyon, S. W.; Nyberg, L.; Rodhe, A.; Bishop, K.; Troch, P. A., Consequences of mixing assumptions for time-variable travel time distributions. Hydrological Processes 2015, 29, (16), 1099-1085,
25   doi:10.1002/hyp.10372.

Voss, M.; Deutsch, B.; Elmgren, R.; Humborg, C.; Kuuppo, P.; Pastuszak, M.; Rolff, C.; Schulte, U., Source identification of nitrate by means of isotopic tracers in the Baltic Sea catchments. Biogeosciences 2006, 3, (4), 663-676, doi:10.5194/bg-3-663-2006.

Wanner, C.; Eggenberger, U.; Mäder, U., A chromate-contaminated site in southern Switzerland – Part 2: Reactive transport
30   modeling to optimize remediation options. Applied Geochemistry 2012, 27, (3), 655-662, doi:10.1016/j.apgeochem.2011.11.008.

Wexler, S. K.; Goodale, C. L.; McGuire, K. J.; Bailey, S. W.; Groffman, P. M., Isotopic signals of summer denitrification in a northern hardwood forested catchment. Proceedings of the National Academy of Sciences 2014, 111, (46), 16413-16418, doi:10.1073/pnas.1404321111.

Wiegert, C.; Aeppli, C.; Knowles, T.; Holmstrand, H.; Evershed, R.; Pancost, R. D.; Macháčková, J.; Gustafsson, Ö., Dual Carbon–Chlorine Stable Isotope Investigation of Sources and Fate of Chlorinated Ethenes in Contaminated Groundwater. Environ. Sci. Technol. 2012, 46, (20), 10918-10925, doi:10.1021/es3016843.

Wittmer, I. K.; Bader, H. P.; Scheidegger, R.; Stamm, C., REXPO: A catchment model designed to understand and simulate the loss dynamics of plant protection products and biocides from agricultural and urban areas. Journal of Hydrology 2016, 533, 486-514, doi:10.1016/j.jhydrol.2015.11.046.

Wu, L.; Yao, J.; Trebse, P.; Zhang, N.; Richnow, H. H., Compound specific isotope analysis of organophosphorus pesticides. Chemosphere 2014, 111, (0), 458-463, doi:10.1016/j.chemosphere.2014.04.037.

Zambrano-Bigiarini, M.; Rojas, R., A model-independent Particle Swarm Optimisation software for model calibration. Environmental Modelling & Software 2013, 43, 5-25.

Zwank, L.; Berg, M.; Elsner, M.; Schmidt, T. C.; Schwarzenbach, R. P.; Haderlein, S. B., New evaluation scheme for two-dimensional isotope analysis to decipher biodegradation processes: Application to groundwater contamination by MTBE. Environ. Sci. Technol. 2005, 39, (4), 1018-1029, doi:10.1021/es049650j.

Table 1. Equations of the hydrological model. See also explanation of parameters in Table 3.

<u>Source zone</u>

Storage

$$\frac{dS_{sz}}{dt} = P - E_{sz} - Q_{sz}$$

Evapotranspiration

$$E_{sz} = \begin{cases} E_{pot} \; if \; E_{pot} \leq S_{sz} \\ S_{sz} \; if \; E_{pot} > S_{sz} \end{cases}$$

Discharge

$$Q_{sz} = \begin{cases} 0 \; if \; P - E_{sz} - (S_{max} - S_{sz}) \leq 0 \\ P - E_{sz} - (S_{max} - S_{sz}) \; otherwise \end{cases}$$

Overland flow[a]

$$OF = \frac{\int_0^{Q_{sz}} N(x|\mu_{OF}, \sigma_{OF})(Q_{sz} - x)dx}{\int_0^{\infty} N(x|\mu_{OF}, \sigma_{OF}) \, dx}$$

<u>Transport zone</u>

Storage

$$\frac{dS_{tz}}{dt} = R_{tz} - E_{tz} - Q_{tz}$$

Recharge

$$R_{tz} = Q_{sz} - OF$$

Evapotranspiration

$$E_{tz} = \begin{cases} min(E_{pot} - E_{sz}, S_{tz}) \; if \; S_{tz} \geq S_{red} \\ min\left(\frac{S_{tz} - S_{red}}{S_{ext} - S_{red}}(E_{pot} - E_{sz}), S_{tz}\right) \; if \; S_{ext} < S_{tz} < S_{red} \\ 0 \; if \; S_{tz} \leq S_{ext} \end{cases}$$

Discharge

$$Q_{tz} = [(2 - b)a(S_{tz} - S_0)]^{\frac{1}{(2-b)}}$$

a $N(x|\mu_{OF}, \sigma_{OF})$ denotes the normal distribution with mean μ_{OF} and standard deviation σ_{OF} evaluated at x (cf. Table 3).

Table 2. Equations of the pesticide model. See also explanation of parameters in Table 3.

	Parameter	Equation
Source zone		
Storage	Change of pesticide mass	$\dfrac{dM_{sz}}{dt} = \phi_{inp} - \phi_{sz} + \phi_{ex} - \phi_{er} - D_{sz}$
Fluxes	Application	ϕ_{inp}
	Via discharge	$\phi_{sz} = Q_{sz}\, C_{sz}$
	Via plant exudation	$\phi_{ex} = f_{ex}\phi_{et}$
	Via erosion	$\phi_{er} = OF\, f_{er}\, M_{sz}$
	Degradation	$D_{sz} = r_0 M_{sz}$
Concentration	Average concentration	$C_0 = \dfrac{M_{sz}}{S_{sz}}$
	In discharge (Q_{sz})	$C_{sz}(t) = \displaystyle\int_0^\infty p_{Q,sz}(T_{sz},t)\, C_0(t - T_{sz})(1 - e^{-lT_{sz}})e^{-r_0 T_{sz}}\, dT_{sz}$
	Probability density function of travel times T_{sz} of pesticide in Q_{sz} at time t	$p_{Q,sz}(T_{sz},t)$

Transport zone		
	Parameter	Equation
Storage	Change of pesticide mass	$\dfrac{dM_{tz}}{dt} = \phi_r - \phi_{et} - \phi_{tz} - D_{tz}$
Fluxes	Via recharge	$\phi_r = R_{tz}\, C_{sz}$
	Via evapotranspiration	$\phi_{et} = E_{tz}\, C_{ET}$
	Via discharge	$\phi_{tz} = Q_{tz}\, C_{tz}$
	Degradation	$D_{tz} = r_0 e^{-kt} M_{tz}$
Concentration	In discharge (Q_{tz})	$C_{tz}(t) = \displaystyle\int_0^\infty p_{Q,tz}(T_{tz},t)\, C_{sz}(t - T_{tz})e^{-\frac{r_0}{k}(1 - e^{-kT_{tz}})}\, dT_{tz}$
	In evapotranspiration (E_{tz})	$C_{ET}(t) = \displaystyle\int_0^\infty p_{ET,tz}(T_{tz},t)\, C_{sz}(t - T_{tz})e^{-\frac{r_0}{k}(1 - e^{-kT_{tz}})}\, dT_{tz}$

Probability density function of travel times T_{tz} of pesticide in Q_{tz} at time t		$p_{Q,tz}(T_{tz}, t)$
Probability density function of travel times T_{tz} of pesticide in E_{tz} at time t		$p_{ET,tz}(T_{tz}, t)$

Stream

Concentration	Dissolved phase	$C_D = \dfrac{C_{tz}\, Q_{tz} + C_{sz}\, OF}{Q_{tz} + OF}$
Carbon isotope ratio	Dissolved phase	$\delta^{13}C_D = \dfrac{{C_D}^{13} / {C_D}^{12}}{\left({}^{C^{13}} / {}_{C^{12}}\right)_{VPDB}} - 1$

Table 3. Parameters of the hydrological and pesticide model with the lower and upper bounds of the parameter values for model calibration.

Parameter	Symbol	Calibration range
Source zone		
Storage capacity [mm]	S_{max}	0.1 – 10
Transport zone		
Mean infiltration capacity [mm d^{-1}]	μ_{OF}	5 – 50
Standard deviation of infiltration capacity [mm d^{-1}]	σ_{OF}	0.05 – 25
First fitting parameter of storage-discharge relation [-]	a	0.05 – 0.1
Second fitting parameter of storage-discharge relation [-]	b	1 – 1.8
Storage for which discharge from transport zone ceases [mm]	S_0	30 – 100
Storage for which ET from transport zone starts to reduce [mm]	S_{red}	25 – 320
Storage for which ET from transport zone ceases [mm]; constrained to below S_{red}	S_{ext}	15 – 120
Calculation of travel time distributions		
Preference for young (<1) or old (>1) water in discharge from transport zone during dry periods [-]	α_Q	0.2 – 1.9
Change fraction of α_Q from the driest to the wettest conditions[a] [-]	β_Q	0 – 0.95
Preference for young water in ET from transport zone [-]	α_{ET}	0.01 – 0.8
Pesticide model		0.95 – 1.05
Calibration factor for applied pesticide mass [-]	m_{IN}	
Degradation rate constant [1 d^{-1}]	r_0	0.02 – 0.14
Coefficient for decrease of degradation rate constant in transport zone with travel time [1 d^{-1}]	k	$5.0 \cdot 10^{-3}$ – 0.03
Coefficient describing pesticide sorption in the source zone [1 d^{-1}]	l	0.05 – 0.37
Fraction of pesticide transfer from transport to source zone via ET and plant exudation [-]	f_{ex}	0.01 – 0.5
Eroded fraction of pesticide mass in the source zone via overland flow [1 mm^{-1}]	f_{er}	$3.4 \cdot 10^{-4}$ – 0.02
Isotopic enrichment factor [‰]	ε_C	-5 – -0.5
Carbon isotope ratio of the applied pesticide product [‰]	$\delta^{13}C_0$	fixed at -32.5

[a] VIM model; van der Velde et al. (2015)

Table 4: Model mass-balance for degraded and transported pesticide in 2011, 2012, and the study period (12 April to 17 July). Numbers are relative to the annually applied pesticide mass.

	Study period[a]	2012	2011
Degradation [%]	**74.7±9.5[b]**	**92.6±-5.9**	**95.3±2.6**
Source zone [%]	71.3±9.6	80.8±6.5	90.2±4.5
Transport zone [%]	3.4±1.9	11.8±5.0	5.2±2.3
Transport to catchment outlet [%]	**4.6±5.3**	**4.7±5.3**	**0.2±0.7**
Overland flow [%]	0.5±0.4	0.5±0.4	0
Eroded [%]	3.8±5.2	3.8±5.2	0.1±0.6
Discharge from transport zone [%]	0.3±0.2	0.4±0.2	0.1±0.1
Total [%]	**79.3±8.2**	**97.3±2.0**	**95.6±2.5**
Pesticide retention [%]	**20.7±8.2**	**2.7±2.0**	**4.4±2.5**

[a] 12 April to 17 July: from first application of S-metolachlor to last sampling day for CSIA

[b] mean ± standard deviation of all runs
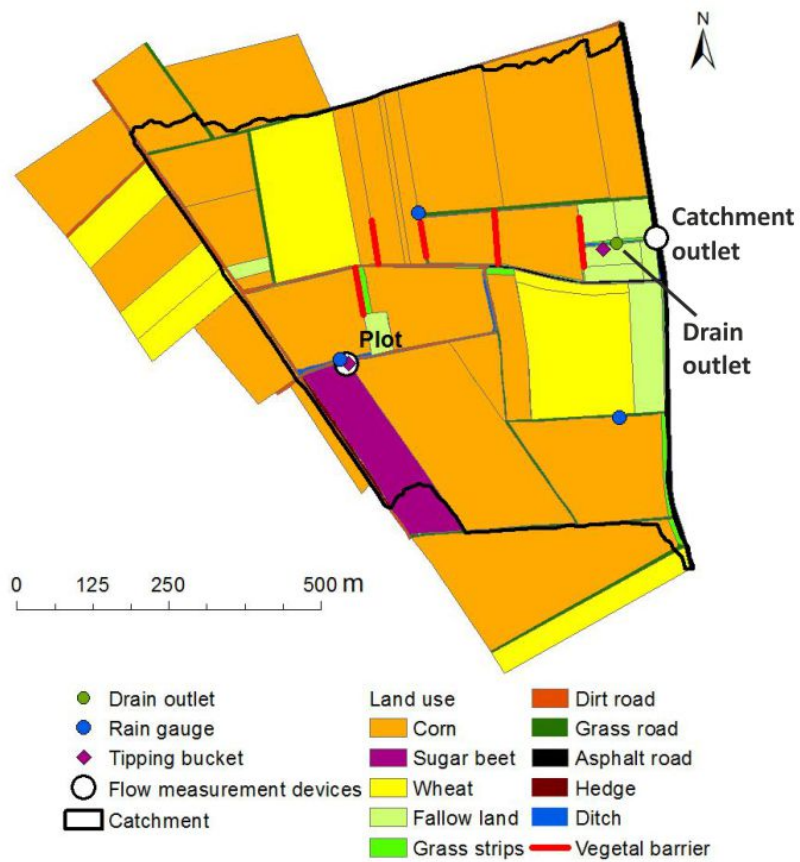
Figure 1: Scheme of the Alteckendorf catchment (Bas-Rhin, France) with land cover and crop types. Samples were taken at the plot outlet, drain outlet and catchment outlet.

5

Hydrological model

R_S	Incoming solar radiation
P	Precipitation
S_{sz}	Source zone storage
S_{tz}	Transport zone storage
E_{sz}	Evapotranspiration from source zone
Q_{sz}	Discharge from source zone
O_F	Overland flow to catchment outlet
R_{tz}	Recharge to transport zone
Q_{tz}	Discharge from transport zone
E_{tz}	Evapotranspiration from transport zone
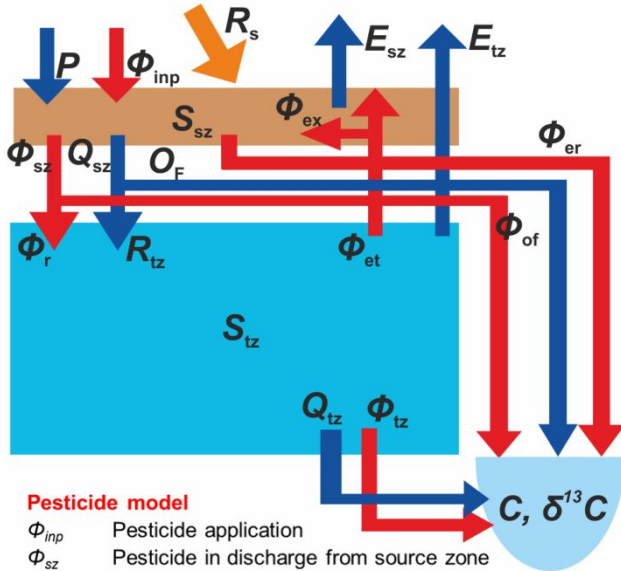
Pesticide model

Φ_{inp}	Pesticide application
Φ_{sz}	Pesticide in discharge from source zone
Φ_{of}	Pesticide in overland flow
Φ_{er}	Pesticide transport via erosion (particulate phase)
Φ_r	Pesticide in recharge to transport zone
Φ_{et}	Pesticide in evapotranspiration from transport zone
Φ_{ex}	Pesticide in plant exudation
Φ_{tz}	Pesticide in discharge from transport zone
C	Pesticide concentration at catchment outlet
$\delta^{13}C$	Carbon isotope ratio of pesticide at catchment outlet

Figure 2: Model scheme showing water flow (blue arrows) and pesticide transport routes (red arrows) from the source zone (brown box) and transport zone (blue box) to the catchment outlet (light blue semi-circle).
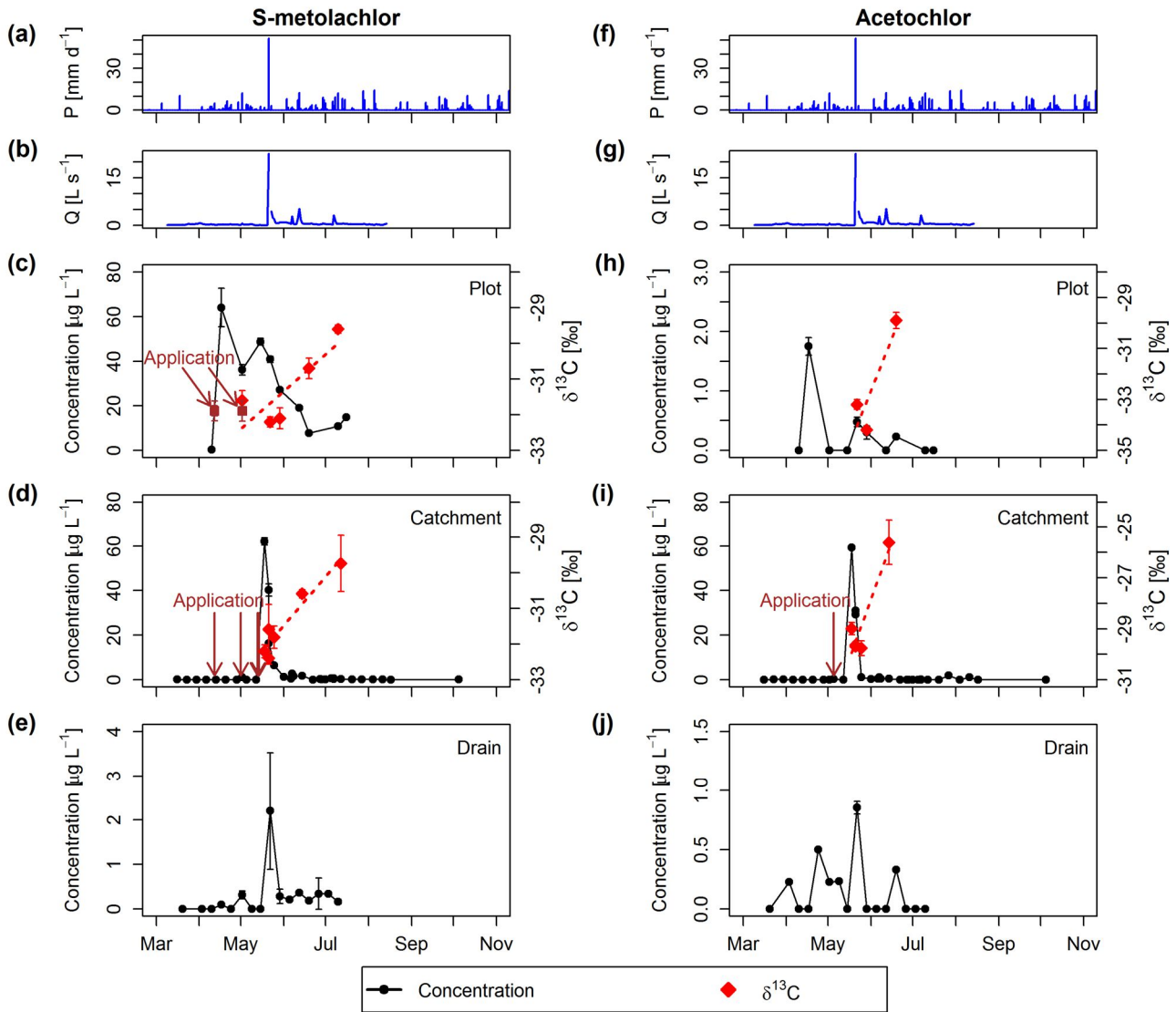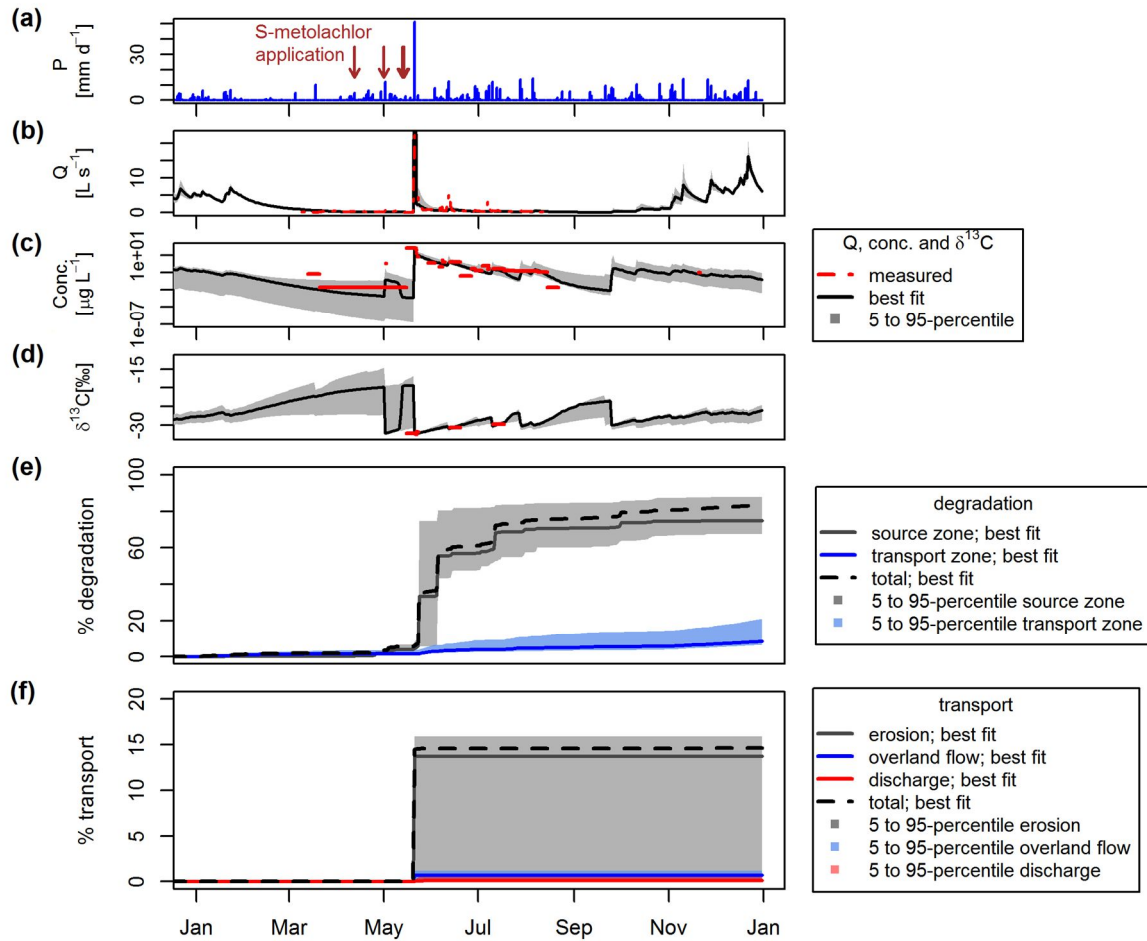
Figure 3: Measured precipitation (P, panels a and f), discharge (Q, panels b and g), concentrations (black dots) and δ¹³C-values (red diamonds) of S-metolachlor (left panels) and acetochlor (right panels) at the plot (c, h), catchment outlet (d, i) and drain outlet (e, j). Standard deviations of replicate measurements are indicated by vertical error bars. Linear regression of δ¹³C-values is shown as dashed red lines (coefficients of determination: R^2 = 0.70 (c), R^2 = 0.92 (d), R^2 = 0.80 (h), and R^2 = 0.86 (i)). Dates of reported pesticide application in the study catchment are indicated in brown (including the δ¹³C-values of the applied pesticide in the plot experiment in panel c).
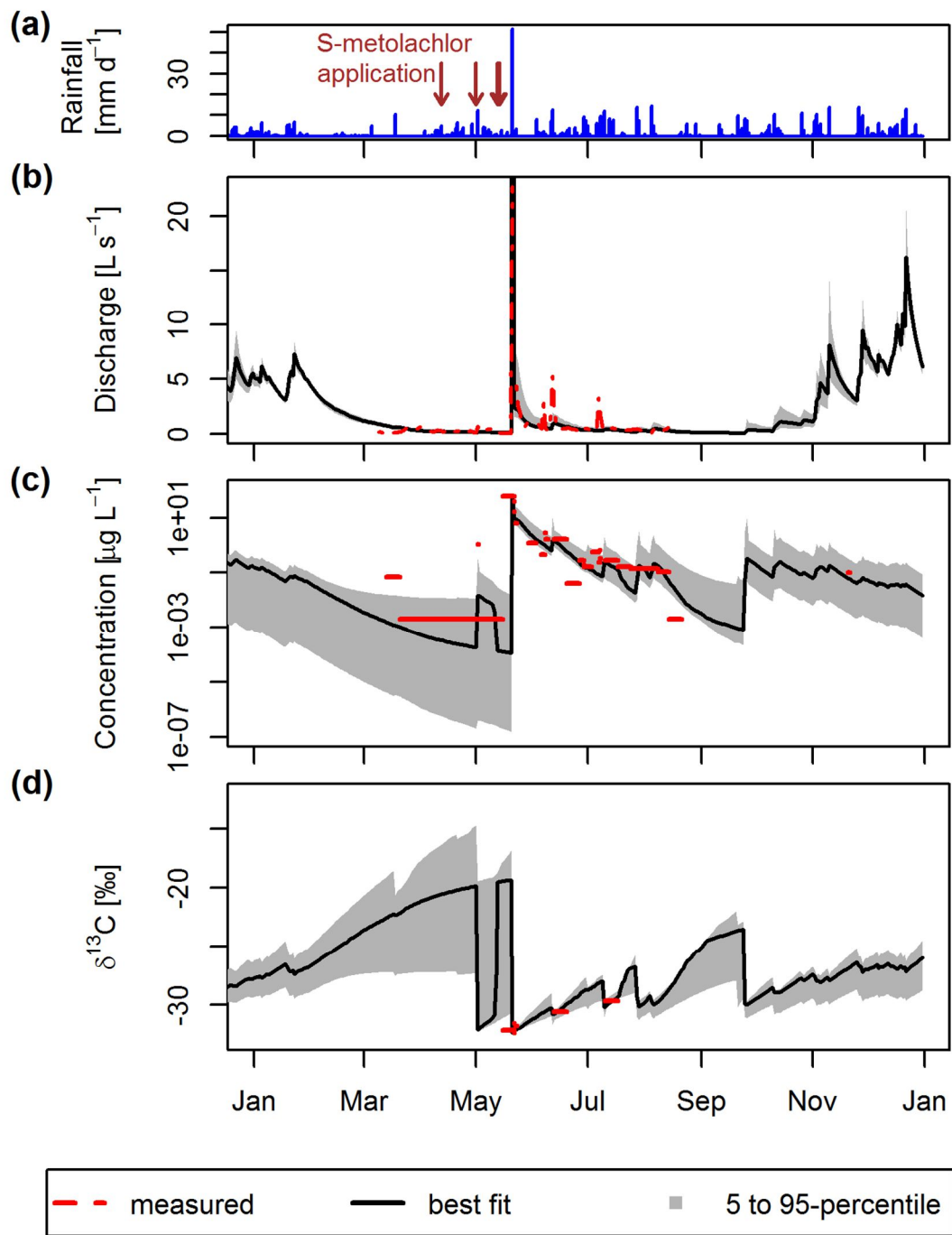
Figure 4: Daily precipitation (a), and measured (red lines) and modelled time series for discharge (b), S-metolachlor concentrations (c; note the log-scaling) and δ13C-values (d) at the catchment outlet in 2012. The black line indicates the results of the calibration run with the best fit in terms of the mean of $N_Q/6$, N_C, and $N_{δ13C}$. Shaded areas show the range between the 5- and 95-percentiles of all simulation results. Brown arrows in (a) indicate the dates of pesticide application.

Figure 5: Daily precipitation (P; panel a), measured (red lines) and modelled time series for discharge (Q; panel b), S-metolachlor concentrations (c; note the log-scaling) and δ^{13}C-values (d) at the catchment outlet in 2012, and model mass-balance for degradation (e) and transport processes (f) within the catchment. The black line indicates the results of the calibration run with the best fit in terms of the mean of $N_Q/6$, N_C, and $N_{δ13C}$. Shaded areas show the range between the 5- and 95-percentiles of all simulation results. Brown arrows in (a) indicate the dates of pesticide application.
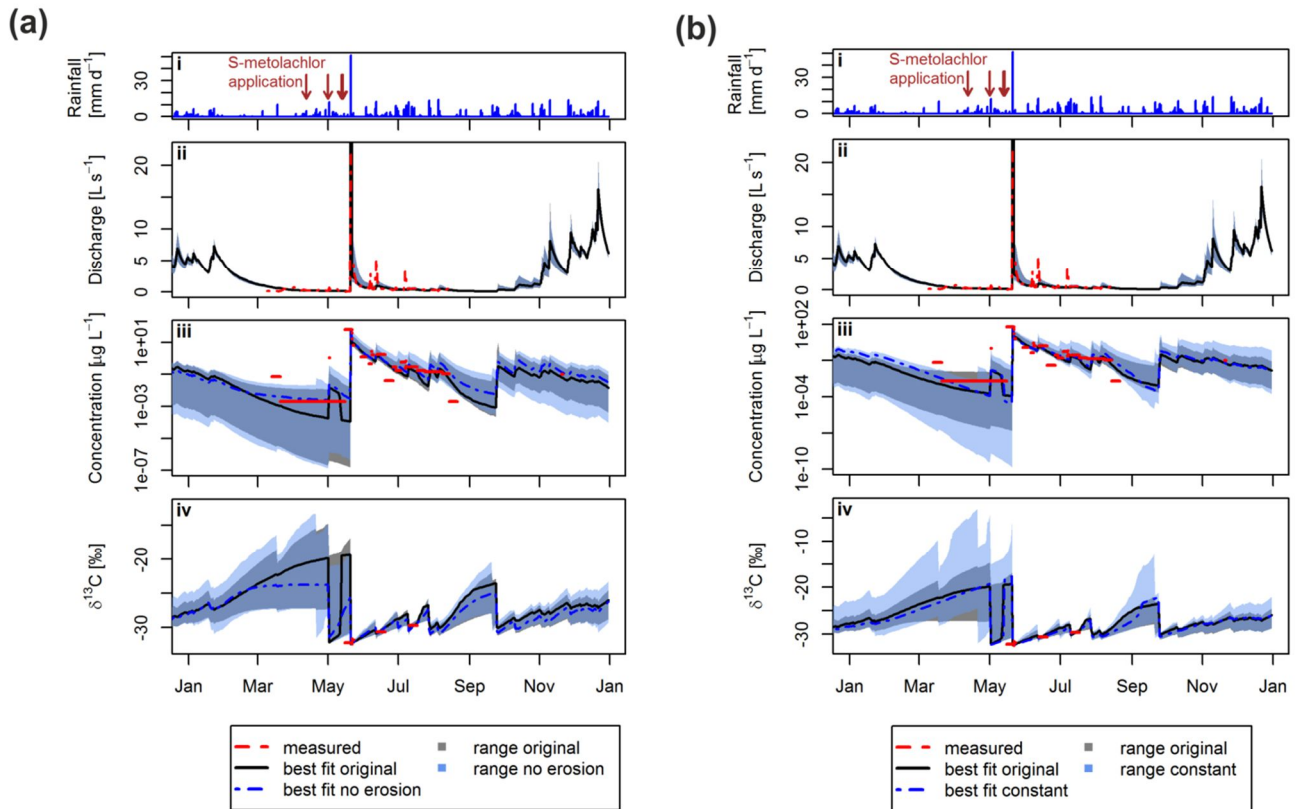
Figure 6: Comparison between the original model and modified model setups: without erosion (a) and with a constant degradation half-life in the transport zone (b), respectively. Measured (red lines) and modelled time series are given for discharge (a, ii and b, ii), S-metolachlor concentrations (a, iii and b, iii; note the log-scaling) and δ^{13}C-values (a, iv and b, iv) in 2012. Best-fit simulations for the modified and original model setups are indicated as dashed blue and solid black lines, respectively. Shaded areas show the range between the 5- and 95-percentiles of 1000 calibration runs with the modified models (transparent blue) and 10,000 calibration runs with the original model (dark grey), respectively. Blue bars in (a, i and b, i) indicate daily precipitation and brown arrows indicate the dates of pesticide application.
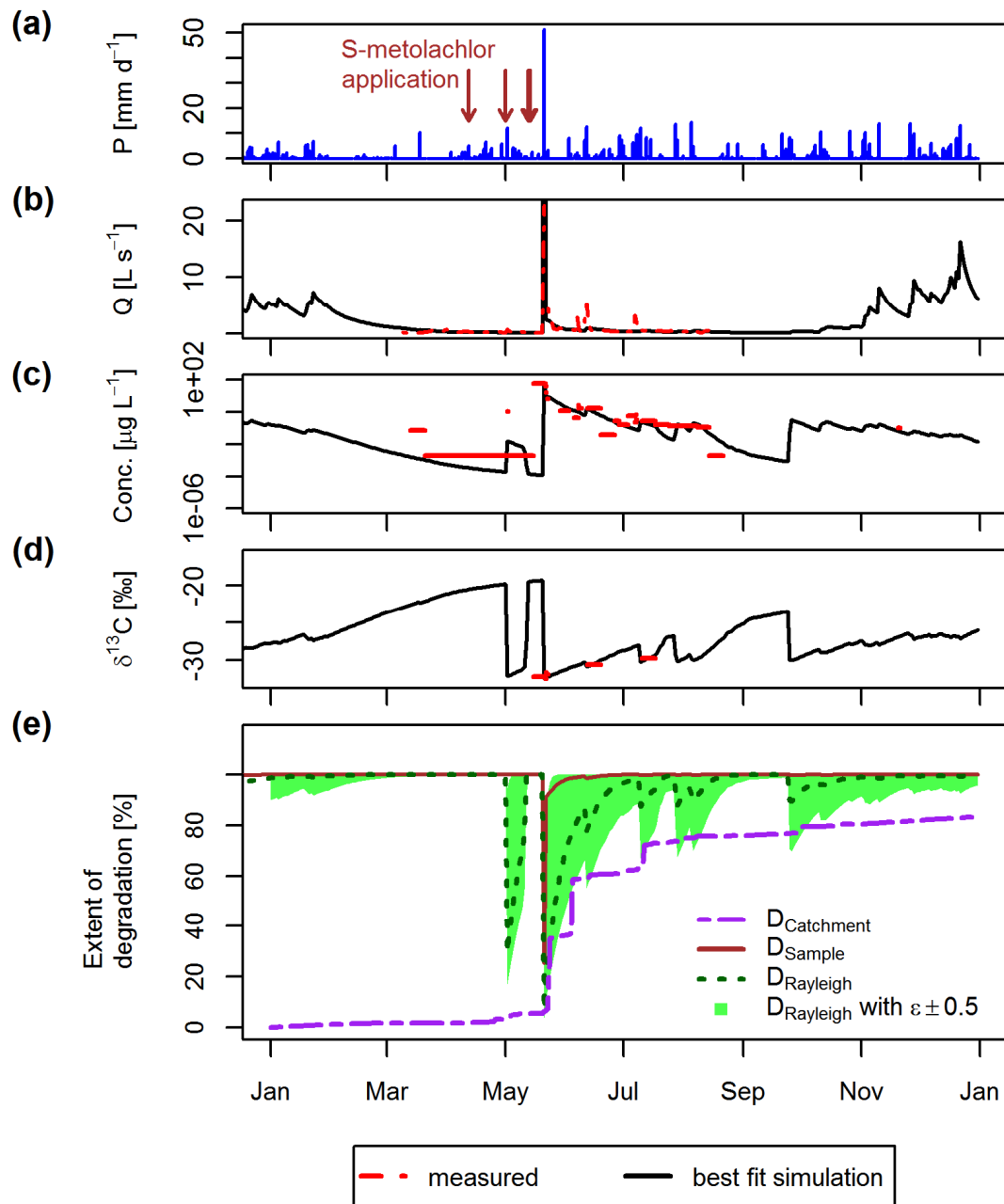
Figure 7: Measured (red lines) and modelled time series (black lines; best-fit simulation) for discharge (b), S-metolachlor concentrations (c; note the log-scaling) and δ^{13}C-values (d), and extent of degradation as obtained by the Rayleigh equation ($D_{Rayleigh}$, dotted green line; range of $D_{Rayleigh}$ for $\varepsilon_C = -1.13\pm0.5$ ‰, green area) and as known from the model for the sample (D_{Sample}, solid brown line) and for the entire catchment ($D_{Catchment}$, dashed purple line; e). Blue bars in (a) indicate daily precipitation and brown arrows indicate the dates of pesticide application.